Renal adaptive response to exposure to low doses of uranyl nitrate and sodium fluoride in mice

Alice Bontemps, Victor Magneron, Laurine Conquet, Christelle Elie, Celine Gloaguen, Dimitri Kerezelidze, Laurence Roy, Olivier Barbier, Yann Gueguen

Journal of Trace Elements in Medicine and Biology

Renal adaptive response to exposure to low doses of uranyl nitrate and sodium fluoride in mice

--Manuscript Draft--

Manuscript Number:	JTEMB-D-20-00473R1
Article Type:	Research Paper
Section/Category:	Toxicology
Keywords:	uranyl; fluoride; Kidney; adaptation; Apoptosis; Inflammation
Corresponding Author:	Yann GUEGUEN, Ph.D. Institut de radioprotection et de Sûreté Nucléaire Fontenay-aux-Roses, Île-de-France FRANCE
First Author:	Alice Bontemps-Karcher
Order of Authors:	Alice Bontemps-Karcher
	Victor Magneron
	Laurine Conquet
	Christelle Elie
	Céline Gloaguen
	Dimitri Kereselidze
	Laurence Roy
	Olivier C. Barbier
	Yann GUEGUEN, Ph.D.
Abstract:	BACKGROUND: Despite their differences in physicochemical properties, both uranium (U) and fluoride (F) are nephrotoxicants at high doses but their adverse effects at low doses are still the subject of debate. METHODS: This study aims to improve the knowledge of the biological mechanisms involved through an adaptive response model of C57BL/6J mice chronically exposed to low priming doses of U (0, 10, 20 and 40 mg/L) or F (0, 15, 30 and 50 mg/L) and then challenged with acute exposure of 5 mg/kg U or 7.5 mg/kg NaF. RESULTS: We showed that an adaptive response occurred with priming exposures to 20 mg/L U and 50 mg/L F, with decreased levels of the biomarkers KIM-1 and CLU compared to those in animals that received the challenge dose only (positive control). The adaptive mechanisms involved a decrease in caspase 3/7 activities in animals exposed to 20 mg/L U and a decrease in in situ VCAM expression in mice exposed to 50 mg/L F. However, autophagy and the UPR were induced independently of priming exposure to U or F and could not be identified as adaptive mechanisms to U or F. CONCLUSION: Taken together, these results allow us to identify renal adaptive responses to U and F at doses of 20 and 50 mg/L, probably through decrease apoptosis and inflammatory cell recruitment.
Suggested Reviewers:	Mara Medeiros Domingo, PhD Hospital Infantil de Mexico Federico Gomez maramedeiros@hotmail.com Expertise in fluoride toxicity
	Armelle Baeza, PhD Université Paris Diderot-Paris 7 baeza@univ-paris-diderot.fr Expertise in adaptive response
	Edward Azzam, PhD Rutgers New Jersey Medical School azzamei@njms.rutgers.edu Expertise in low dose ionizing radiation, radiation-induced bystander effect and the radiation-induced adaptive response

	Edward Calabrese, PhD University of Massachusetts Amherst edwardc@schoolph.umass.edu Expertise in toxicology, risk assessment, environmental health, dose response, hormesis
Response to Reviewers:	

Highlights :

- Uranium and fluoride induce an adaptive response in mice exposed chronically
- Apoptosis regulation is involved in uranium-induced adaptive response
- Inflammatory control is involved in fluoride-induced adaptive response
- Uranium induces UPR and autophagy in the kidney
- Fluoride induces UPR in the kidney

Graphical Abstract

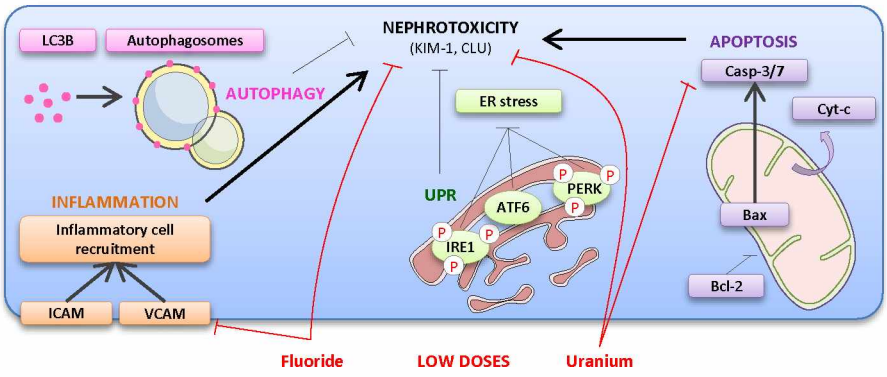

Figure 1

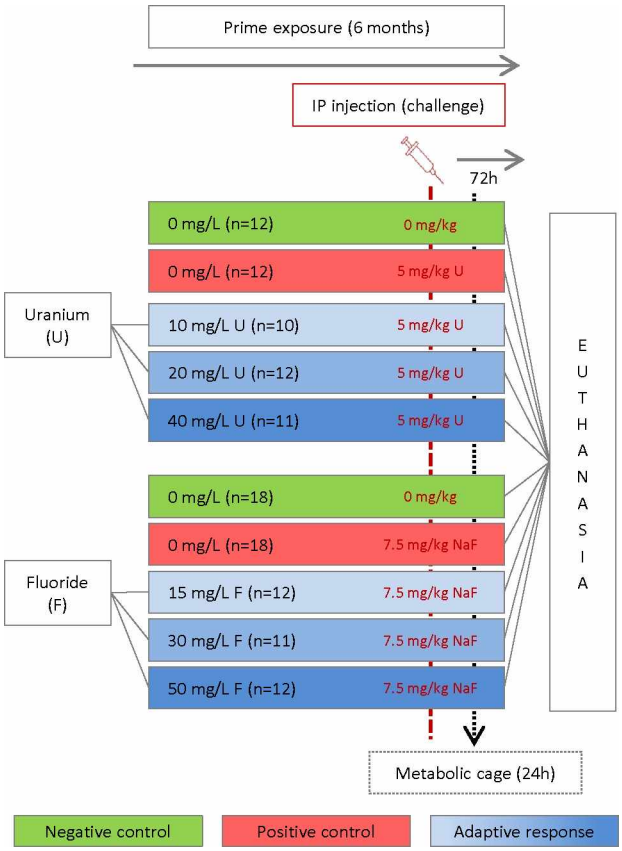
Prime exposure (6 months)
IP injection (challenge)
72h
0 mg/L (n=12)
0 mg/kg
0 mg/L (n=12)
5 mg/kg U
Uranium (U)
10 mg/L U (n=10)
5 mg/kg U
20 mg/L U (n=12)
5 mg/kg U
40 mg/L U (n=11)
5 mg/kg U
0 mg/L (n=18)
0 mg/kg
0 mg/L (n=18)
7.5 mg/kg NaF
Fluoride (F)
15 mg/L F (n=12)
7.5 mg/kg NaF
30 mg/L F (n=11)
7.5 mg/kg NaF
50 mg/L F (n=12)
7.5 mg/kg NaF
EUTHANASIA
Metabolic cage (24h)
Negative control
Positive control
Adaptive response

Figure 2

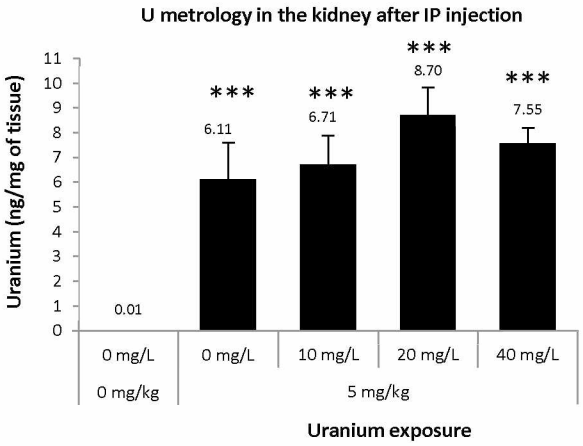
U metrology in the kidney after IP injection
Uranium (ng/mg of tissue)
11
10
9
8
7
6
5
4
3
2
1
0
0.01
6.11
6.71
8.70
7.55
***
***
***
***
0 mg/L
0 mg/kg
0 mg/L
10 mg/L
20 mg/L
40 mg/L
5 mg/kg
Uranium exposure

Figure 3

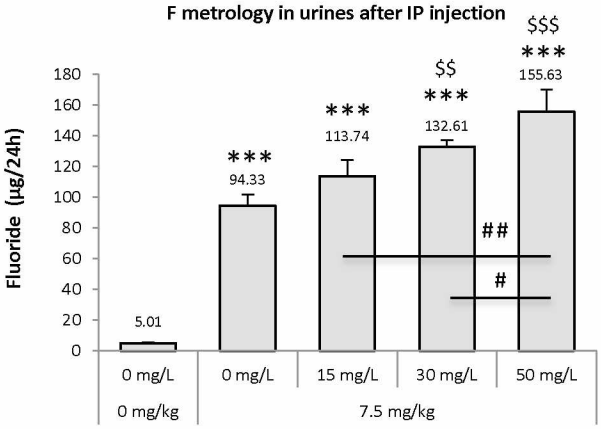
F metrology in urines after IP injection
Fluoride (µg/24h)
180
160
140
120
100
80
60
40
20
0
5.01
***
94.33
***
113.74
$$
***
132.61
$$$
***
155.63
##
#
0 mg/L
0 mg/kg
0 mg/L
15 mg/L
30 mg/L
50 mg/L
7.5 mg/kg

Figure 4

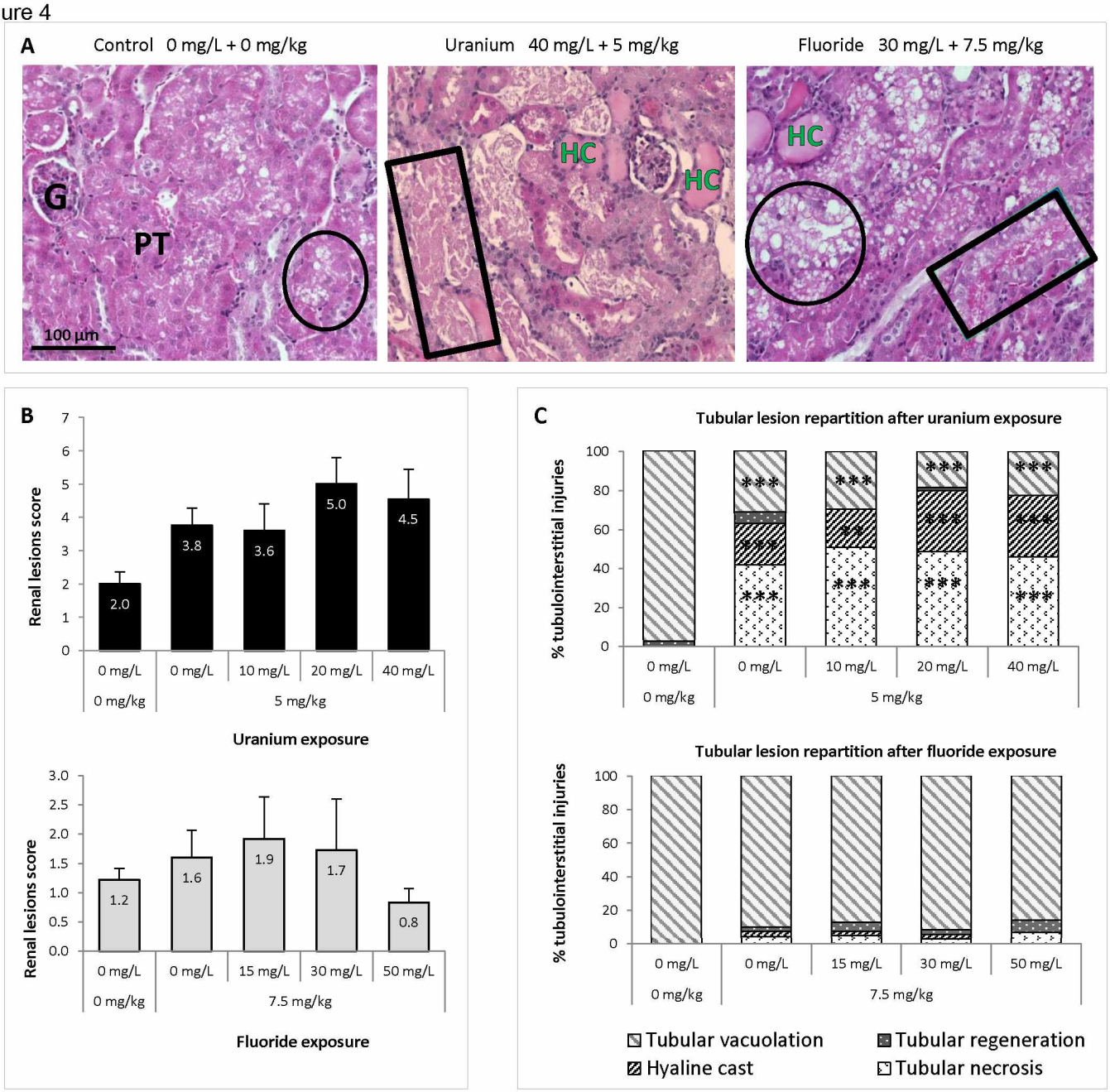
A
Control 0 mg/L + 0 mg/kg
Uranium 40 mg/L + 5 mg/kg
Fluoride 30 mg/L + 7.5 mg/kg
G
PT
HC
HC
HC
100 µm
B
Renal lesions score
2.0
3.8
3.6
5.0
4.5
0 mg/L
0 mg/kg
0 mg/L
10 mg/L
20 mg/L
40 mg/L
5 mg/kg
Uranium exposure
Renal lesions score
1.2
1.6
1.9
1.7
0.8
0 mg/L
0 mg/kg
0 mg/L
15 mg/L
30 mg/L
50 mg/L
7.5 mg/kg
Fluoride exposure
C
Tubular lesion repartition after uranium exposure
% tubulointerstitial injuries
0 mg/L
0 mg/kg
0 mg/L
10 mg/L
20 mg/L
40 mg/L
5 mg/kg
Tubular lesion repartition after fluoride exposure
% tubulointerstitial injuries
0 mg/L
0 mg/kg
0 mg/L
15 mg/L
30 mg/L
50 mg/L
7.5 mg/kg
Tubular vacuolation
Tubular regeneration
Hyaline cast
Tubular necrosis

Figure 5

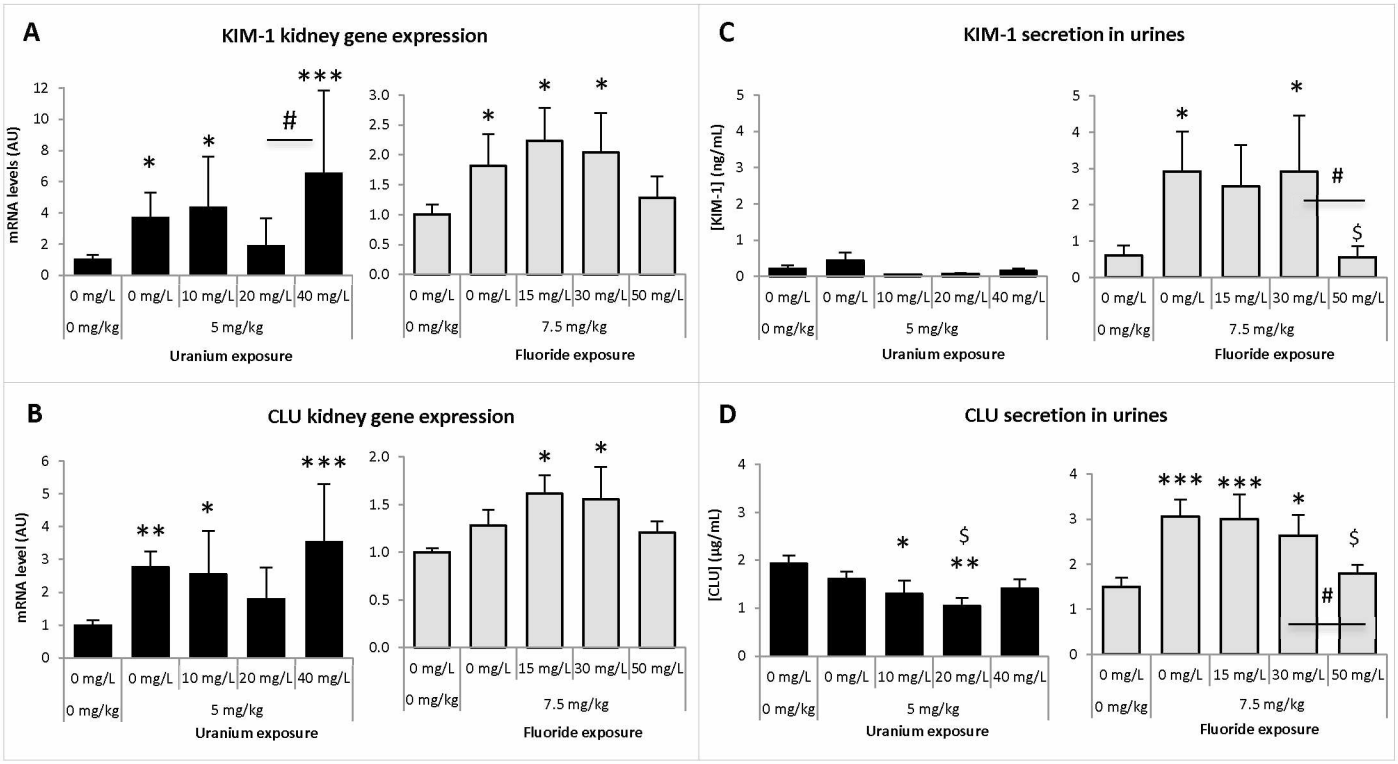
A
KIM-1 kidney gene expression
mRNA levels (AU)
0 mg/L
0 mg/L
10 mg/L
20 mg/L
40 mg/L
0 mg/kg
5 mg/kg
Uranium exposure
0 mg/L
0 mg/L
15 mg/L
30 mg/L
50 mg/L
0 mg/kg
7.5 mg/kg
Fluoride exposure
B
CLU kidney gene expression
mRNA level (AU)
C
KIM-1 secretion in urines
[KIM-1] (ng/mL)
D
CLU secretion in urines
[CLU] (µg/mL)

Figure 6

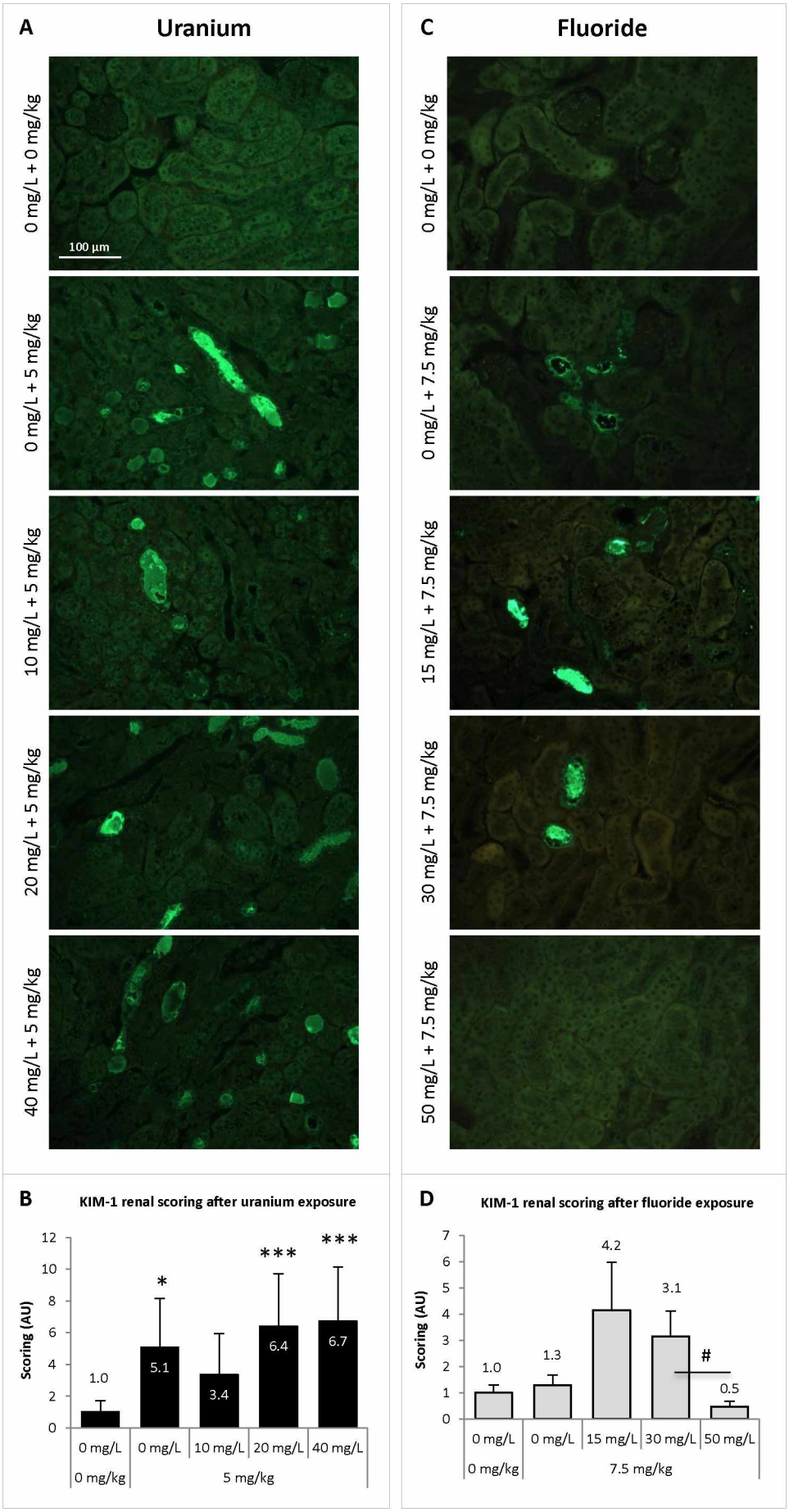
A
Uranium
0 mg/L + 0 mg/kg
100 µm
0 mg/L + 5 mg/kg
10 mg/L + 5 mg/kg
20 mg/L + 5 mg/kg
40 mg/L + 5 mg/kg
C
Fluoride
0 mg/L + 0 mg/kg
0 mg/L + 7.5 mg/kg
15 mg/L + 7.5 mg/kg
30 mg/L + 7.5 mg/kg
50 mg/L + 7.5 mg/kg
B
KIM-1 renal scoring after uranium exposure
Scoring (AU)
12
10
8
6
4
2
0
1.0
5.1
3.4
6.4
6.7
*
***
***
0 mg/L
0 mg/kg
0 mg/L
10 mg/L
20 mg/L
40 mg/L
5 mg/kg
D
KIM-1 renal scoring after fluoride exposure
Scoring (AU)
7
6
5
4
3
2
1
0
1.0
1.3
4.2
3.1
0.5
#
0 mg/L
0 mg/kg
0 mg/L
15 mg/L
30 mg/L
50 mg/L
7.5 mg/kg

Figure 7

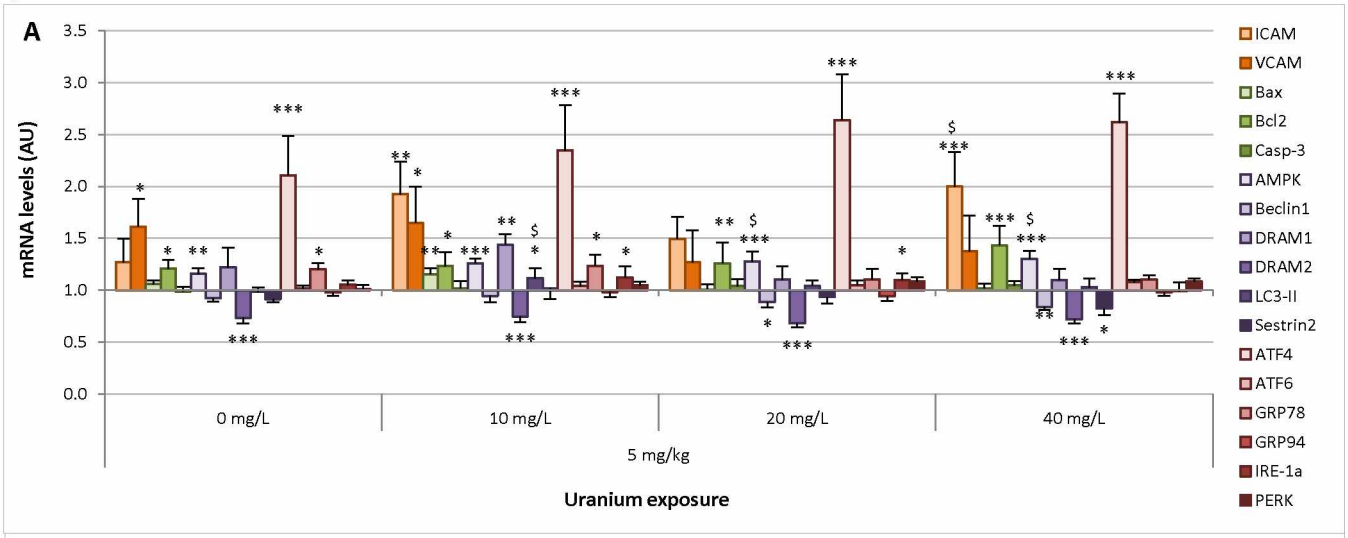
A
mRNA levels (AU)
3.5
3.0
2.5
2.0
1.5
1.0
0.5
0.0
0 mg/L
10 mg/L
20 mg/L
40 mg/L
5 mg/kg
Uranium exposure
ICAM
VCAM
Bax
Bcl2
Casp-3
AMPK
Beclin1
DRAM1
DRAM2
LC3-II
Sestrin2
ATF4
ATF6
GRP78
GRP94
IRE-1a
PERK

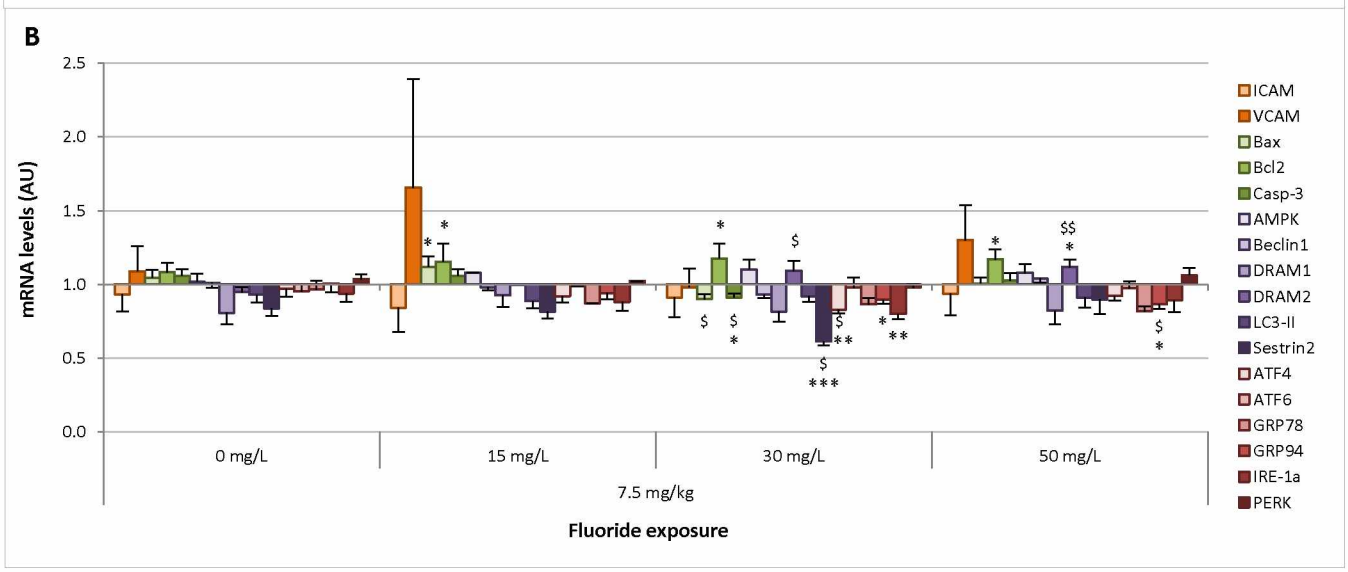
B
mRNA levels (AU)
2.5
2.0
1.5
1.0
0.5
0.0
0 mg/L
15 mg/L
30 mg/L
50 mg/L
7.5 mg/kg
Fluoride exposure
ICAM
VCAM
Bax
Bcl2
Casp-3
AMPK
Beclin1
DRAM1
DRAM2
LC3-II
Sestrin2
ATF4
ATF6
GRP78
GRP94
IRE-1a
PERK

Figure 8

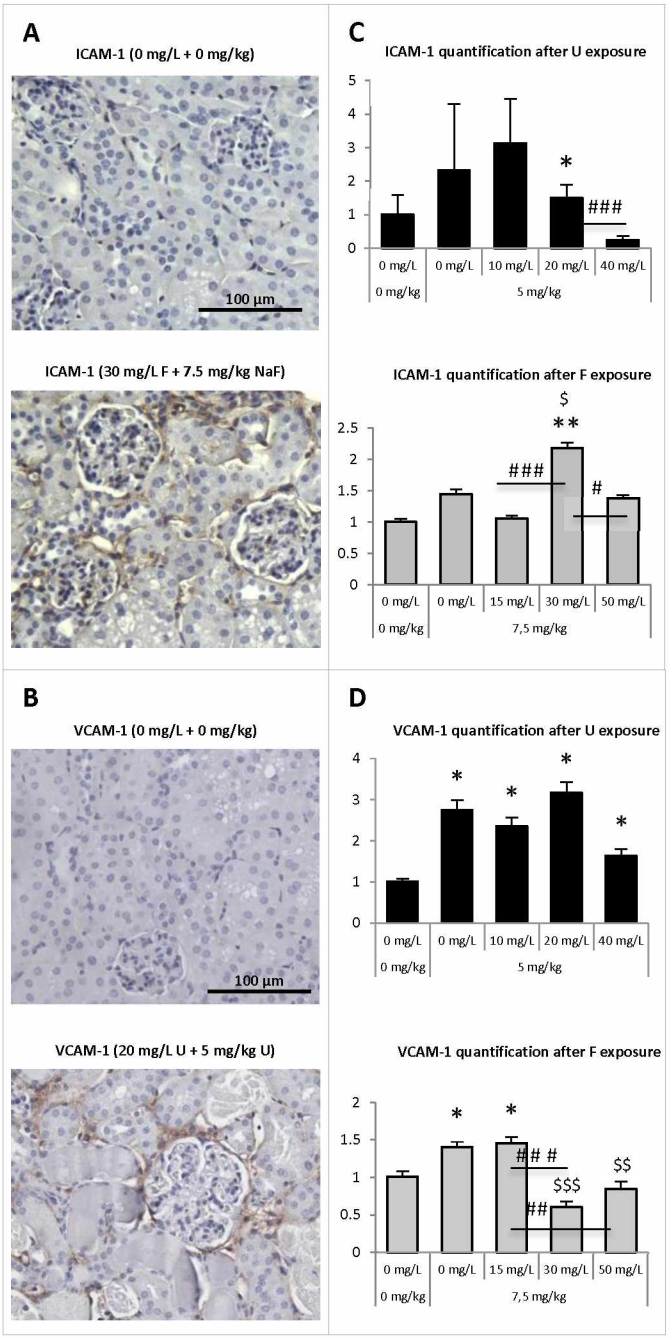
A
ICAM-1 (0 mg/L + 0 mg/kg)
100 µm
ICAM-1 (30 mg/L F + 7.5 mg/kg NaF)
C
ICAM-1 quantification after U exposure
0 mg/L
0 mg/L
10 mg/L
20 mg/L
40 mg/L
0 mg/kg
5 mg/kg
ICAM-1 quantification after F exposure
0 mg/L
0 mg/L
15 mg/L
30 mg/L
50 mg/L
0 mg/kg
7,5 mg/kg
B
VCAM-1 (0 mg/L + 0 mg/kg)
100 µm
VCAM-1 (20 mg/L U + 5 mg/kg U)
D
VCAM-1 quantification after U exposure
VCAM-1 quantification after F exposure

Figure 9

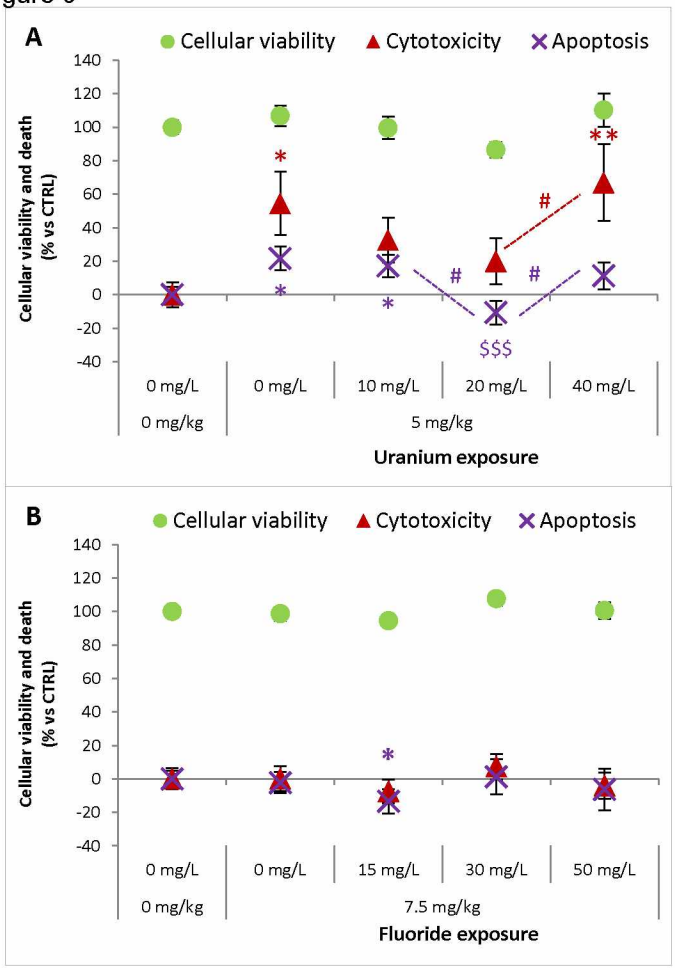
A
Cellular viability
Cytotoxicity
Apoptosis
Cellular viability and death (% vs CTRL)
140
120
100
80
60
40
20
0
-20
-40
*
**
#
#
#
*
*
$$$
0 mg/L
0 mg/kg
0 mg/L
10 mg/L
20 mg/L
40 mg/L
5 mg/kg
Uranium exposure
B
Cellular viability
Cytotoxicity
Apoptosis
Cellular viability and death (% vs CTRL)
140
120
100
80
60
40
20
0
-20
-40
*
0 mg/L
0 mg/kg
0 mg/L
15 mg/L
30 mg/L
50 mg/L
7.5 mg/kg
Fluoride exposure

Figure 10

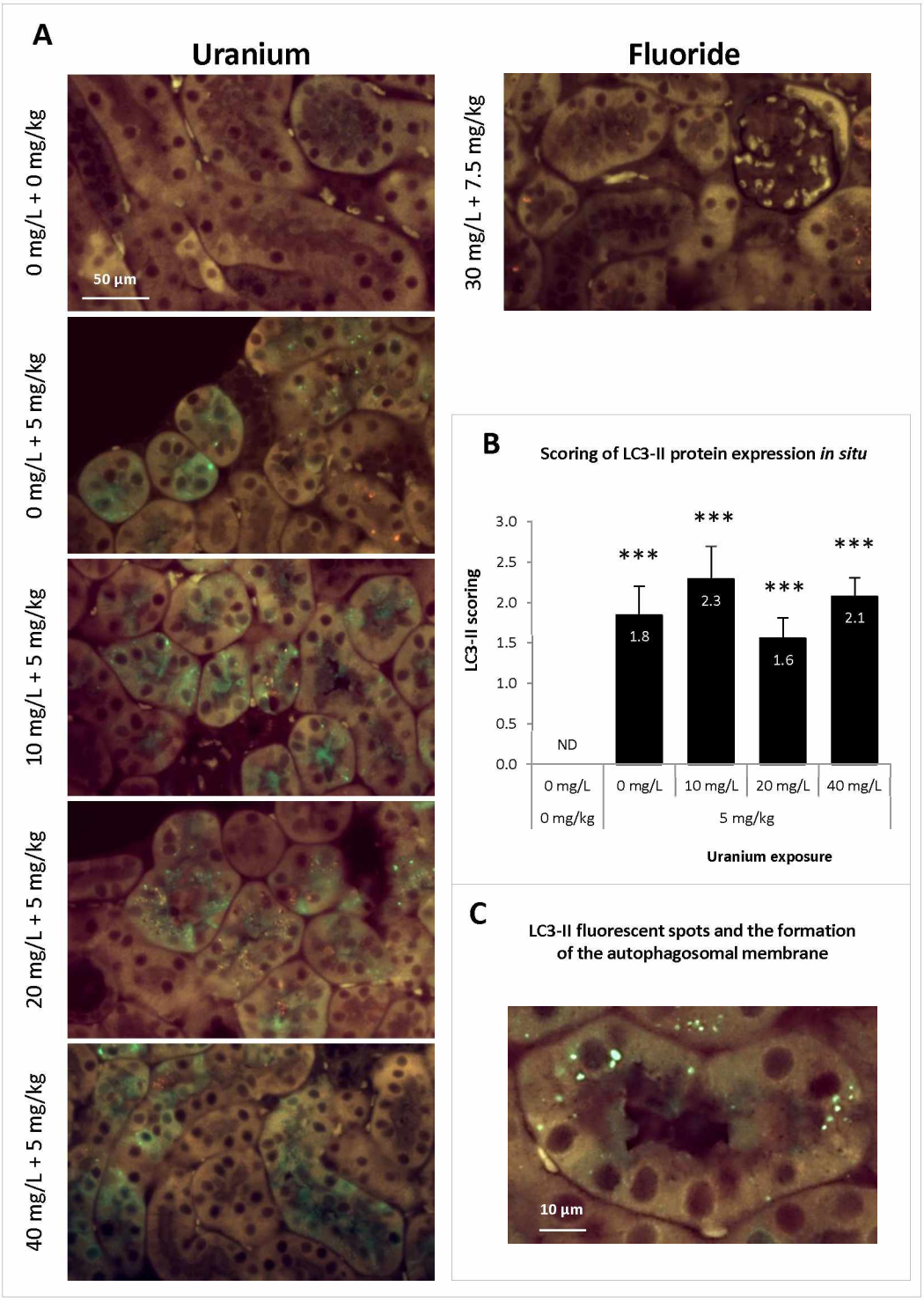
A
Uranium
Fluoride
0 mg/L + 0 mg/kg
30 mg/L + 7.5 mg/kg
50 µm
0 mg/L + 5 mg/kg
10 mg/L + 5 mg/kg
20 mg/L + 5 mg/kg
40 mg/L + 5 mg/kg
B
Scoring of LC3-II protein expression in situ
LC3-II scoring
3.0
2.5
2.0
1.5
1.0
0.5
0.0
***
***
***
***
1.8
2.3
1.6
2.1
ND
0 mg/L
0 mg/L
10 mg/L
20 mg/L
40 mg/L
0 mg/kg
5 mg/kg
Uranium exposure
C
LC3-II fluorescent spots and the formation of the autophagosomal membrane
10 µm

Figure 11

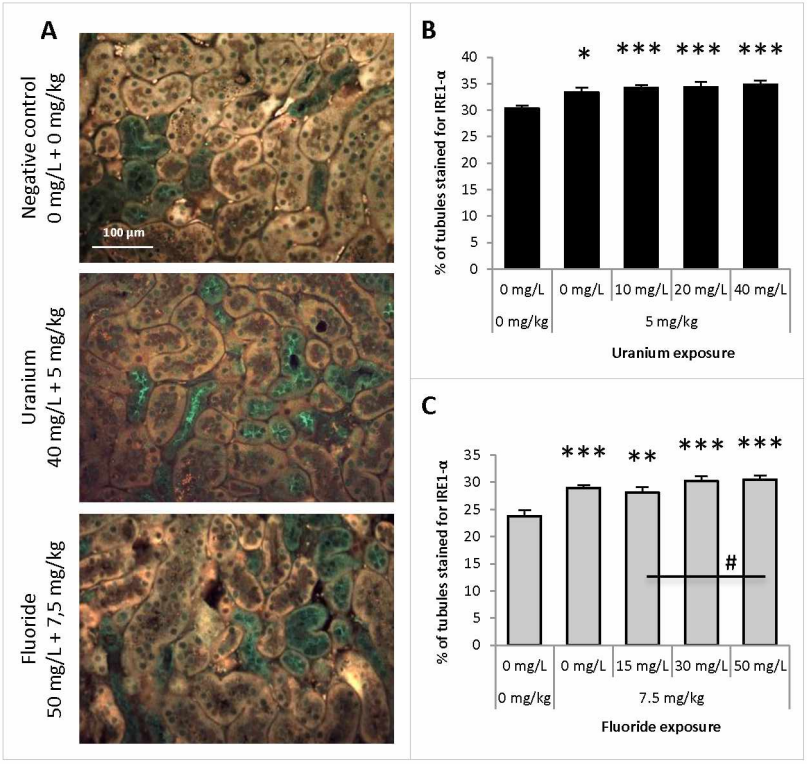
A
Negative control
0 mg/L + 0 mg/kg
100 µm
Uranium
40 mg/L + 5 mg/kg
Fluoride
50 mg/L + 7,5 mg/kg
B
% of tubules stained for IRE1-α
*
***
***
***
0 mg/L
0 mg/L
10 mg/L
20 mg/L
40 mg/L
0 mg/kg
5 mg/kg
Uranium exposure
C
% of tubules stained for IRE1-α
***
**
***
***
#
0 mg/L
0 mg/L
15 mg/L
30 mg/L
50 mg/L
0 mg/kg
7.5 mg/kg
Fluoride exposure

Author contributions

A.B. and Y.G. proposed the concept of the manuscript and designed the experimental study. A.B., Y.G. applied for research ethics approval. A.B., L.C., C.E., V.M., C.G., D.K. and Y.G. performed the experiments and collected data. All authors contributed to data analyses and interpretation. A.B. and Y.G. wrote the manuscript with intellectual input from L.R. and O.B. All authors read and provided input in finalizing the manuscript. Supervision and project administration was done by Y.G.

Renal adaptive response to exposure to low doses of uranyl nitrate and sodium fluoride in mice

Alice Bontemps-Karcher [1], Victor Magneron [1], Laurine Conquet [1], Christelle Elie [1], Céline Gloaguen [1], Dimitri Kereselidze [1], Laurence Roy [1], Olivier C. Barbier[2] and Yann Guéguen [1]*

[1] Institut de Radioprotection et de Sûreté Nucléaire (IRSN), PSE-SANTE, SESANE, 92262 Fontenay-aux-Roses, France

[2] Centro de Investigación y de Estudios Avanzados del Instituto Politécnico Nacional Departamento de Toxicología (CINVESTAV-IPN), Av. IPN No. 2508 Col., San Pedro Zacatenco, México City, CP 07360, Mexico

* Corresponding author: Yann GUEGUEN

Institut de Radioprotection et de Sureté Nucléaire (IRSN), PSE-SANTE, SESANE, LRSI, Fontenay-aux-Roses, France

B.P. n°17, F 92262 Fontenay-aux-Roses Cedex, France

Ph: +33 - 1 58 35 99 78; Fax: +33 - 1 58 35 84 67

E-mail: yann.gueguen@irsn.fr

Abbreviations:

CLU, clusterin; F, fluoride; KIM-1, kidney injury molecule-1; U, uranium; UN, uranyl nitrate; UPR, unfolded protein response; NMDR, non-monotonic dose-response

Abstract:

BACKGROUND: Despite their differences in physicochemical properties, both uranium (U) and fluoride (F) are nephrotoxicants at high doses but their adverse effects at low doses are still the subject of debate. METHODS: This study aims to improve the knowledge of the biological mechanisms involved through an adaptive response model of C57BL/6J mice chronically exposed to low priming doses of U (0, 10, 20 and 40 mg/L) or F (0, 15, 30 and 50 mg/L) and then challenged with acute exposure of 5 mg/kg U or 7.5 mg/kg NaF. RESULTS: We showed that an adaptive response occurred with priming exposures to 20 mg/L U and 50 mg/L F, with decreased levels of the biomarkers KIM-1 and CLU compared to those in animals that received the challenge dose only (positive control). The adaptive mechanisms involved a decrease in caspase 3/7 activities in animals exposed to 20 mg/L U and a decrease in *in situ* VCAM expression in mice exposed to 50 mg/L F. However, autophagy and the UPR were induced independently of priming exposure to U or F and could not be identified as adaptive mechanisms to U or F. CONCLUSION: Taken together, these results allow us to identify renal adaptive responses to U and F at doses of 20 and 50 mg/L, probably through decrease apoptosis and inflammatory cell recruitment.

Keywords: uranyl; fluoride; kidney; adaptation; apoptosis; inflammation

Introduction

Both uranium (U) and fluoride (F) are environmental and anthropogenic contaminants due to mining, or the use of pesticides in agriculture fields, for example. U and F concentrations can vary greatly from one place to another throughout the world. As an example, high water concentrations of fluoride are found in the northeastern region of Niger, where the concentration reaches 2.07 mg/L in surface waters and 2.42 mg/L in groundwaters [1]. The highest concentrations found in drinking water are 20 mg/L for U in well water of the south of Finland [2, 3] and 30 to 50 mg/L for F in water contaminated by geological sources [4], whereas the world health organization (WHO) recommends maximal concentrations of 30 µg/L U, and 1.5 mg/L F [5, 6].

Once ingested, U and F mainly accumulate in the kidney [7-12], which is the most sensitive organ to U and F because of the nephron's functions of filtration, transport and reabsorption [4, 8, 13, 14]. After high-dose exposure in animals, U- and F-induced kidney lesions are mainly localized in the cortical and juxtaglomerular regions of the kidney, where the proximal convoluted tubules are located [15-19] but the effects of low doses are controversial in epidemiological [10, 20-27] or experimental studies [28-36]. A previous study by our laboratory, showed that chronic exposure to different doses of U, from 1 to 600 mg/L U in drinking water, did not induce any nephrotoxicity in rats despite renal accumulation at a level known to be nephrotoxic when induced acutely (> 3µg/g of kidney tissue) [18]. In this study, Poisson et al. (2014) showed that U even induced antioxidative mechanisms, such as glutathione overexpression, which suggests that renal adaptation occurs in response to chronic exposure to low doses, as also hypothesized in other *in vivo* and *in vitro* studies [37-39]. Chronic exposure to F, from 15 ppm to 100 ppm in rats, induces specific biomarkers of nephrotoxicity [40-43] but it can reduce the nephrotoxicity induced by a second exposure to high dose of

gentamicin in rats [44]. The authors demonstrated that F induces cytoprotective factors such as heat shock protein 72, also suggesting a potential adaptive response.

The non-linear relation or the nonmonotonic dose-response (NMDR) model, stipulates that below a certain level, low doses of radiations or chemicals could be consider beneficial for the organism [45-48]. The adaptive response that can explain this NMDR and the ability of a biological system to exhibit fewer detrimental effects in response to exposure to high dose of a toxicant when it has been pre-exposed to a small priming stress [49]. To study this potential renal adaptation to U and F and improve our understanding of health risks at low levels, an animal model of exposure was used. Chronic priming exposures to low doses of U or F were followed by a challenge treatment, delivered acutely and at moderate nephrotoxic doses. This strategy allowed us to detect the effects triggered by priming exposures to low doses of U and F and to identify some underlying mechanisms.

Materials and Methods

2.1. Animals

The study was performed in 8-week-old male C57BL/6J mice weighing 25 ± 5 g at the beginning of the study provided by Charles River (Saint Germain Nuelles, France). Animals were housed in groups of three under controlled conditions. Three weeks of acclimatization was provided before the beginning of the study. Water and food were supplied *ad libitum*. Body weight was monitored once a week and did not show differences between groups (data not shown). The animals were housed for a 24-h period in metabolic cages every month. The study was approved by the IRSN Animal Care Committee #81 and conducted in accordance with French legislation on the protection of animals used for experimental purposes (EC Directive 2010/63/EU and French Decret 2013–118). All experiments were approved by the Ethics

89 Committee #81 and authorized by the French Ministry of Research under the reference
90 APAFIS#9324-2017031613376362 v1 (internal project number P16-05), delivered on 4 July
91 2017.

92 *2.2. Chronic exposure to and acute exposure with U or F and urine collection*

93 U was obtained as uranyl nitrate (UN) (Merck-Prolabo, Fontenay-sous-bois, France),
94 which had a specific activity of 14×10^3 Bq/g and was composed of 99.74% ^{238}U, 0.26% ^{235}U,
95 and 0.001% ^{234}U. F was obtained as sodium fluoride from Sigma (Saint-Quentin Fallavier,
96 France). Ketamine (Imalgène 1000) and Xylazine (5% Rompun) solutions were obtained from
97 Centravet (Dinan, France). Volvic® mineral water (Volvic) was used for exposure of animals
98 through drinking water due to its low minerals concentration to avoid precipitation. Fluoride
99 level (0.2 mg/L) and uranium level (0.28 µg/L) were measured in Volvic mineral water.

100 The mice were divided into different groups (n=10 to 18 per group), as shown in Figure 1,
101 and were chronically exposed with either U (10, 20, or 40 mg/L) or F (15, 30, or 50 mg/L) in
102 Volvic drinking water for 6 months and then injected acutely with 5 mg/kg UN ($UO_2(NO_3)_2$)
103 or 7.5 mg/kg F (corresponding to 16.6 mg/kg NaF). There was a negative control group, which
104 drank Volvic water during the chronic contamination period and received an ip injection of
105 NaCl, and a positive control group, which drank Volvic water during the chronic contamination
106 period and received an injection of either 5 mg/kg UN or 7.5 mg/kg NaF. For chronic
107 contamination, UN and NaF were diluted in Volvic water, and the drinking solutions were
108 mixed with a magnetic agitator. During the contamination period, water consumption was
109 monitored weekly and do not show differences between groups (data not shown). For the acute
110 injections, UN and NaF were diluted in a NaCl solution and filtered the day of the injection.
111 The animals were then euthanized 72 hours later by exsanguination under anesthesia. The
112 challenge doses and the delay before euthanasia were based on our previous results [28] and on
113 the literature. Previous experiments showed a peak of renal effects 72 hours post-injection of U

114 and toxicity at the dose chosen [15, 30, 31, 34, 50, 51]. The experimental design and the animal
115 grouping are presented in Figure 1.

116 Every month during the chronic contamination period and immediately after the acute
117 injection, the animals were housed individually in metabolic cages (Tecniplast, Decines
118 Charpieu,France) for a 24-hour period to collect urine samples at room temperature without
119 food or water contamination. After collection, the urine samples were subsequently centrifuged
120 at 3000 x g for 2 min at 4°C, and the supernatants were isolated and stored at -80°C.

121 *2.3. Euthanasia and kidney collection*

122 Seventy-two hours after injection, the animals were anaesthetized by an ip injection of
123 100 mg/kg ketamine and 10 mg/kg xylazine and euthanized by exsanguination. Both kidneys
124 were collected, weighed wet and sagittally cut. No differences in kidney weight were found
125 between groups (data not shown). Half of the right kidney was placed in 4% formaldehyde for
126 histopathological analysis, and the other half was used for U or F quantification. The entire left
127 kidney was designated for biomolecular analysis after being flash-frozen in liquid nitrogen and
128 stored at -80°C.

129 *2.4. U and F measurements in the urine and kidney tissues*

130 U was quantified in the kidney by inductively-coupled plasma mass spectrometry
131 (ICP-MS) (ICP-MS, PQ, Excell, Thermo Electron, Villebon-sur-Yvette,France), as previously
132 described [18, 28]. The half-kidney was digested in nitric acid and hydrogen peroxide, and the
133 samples were then evaporated and dissolved in nitric acid. After the appropriate dilution, the U
134 content was measured using bismuth as an internal control and a U calibration curve. The
135 detection limit of U was determined by ICP-MS: 0.5 ng/L for ^{238}U and 0.01 ng/L for ^{235}U. After
136 dilution, F was quantified in the urine by a potentiometric method using an ion selective
137 electrode (Thermo Scientific Orion, Villebon-sur-Yvette, France).

138 *2.5. Histopathology and immunostaining*

139 After 24 hours in 4% formaldehyde, the preserved half-kidney was dehydrated before
140 being embedded in paraffin and cut into 5 µm slices with a microtome. Hematoxylin, eosin,
141 and saffron (HES) staining was conducted, and the slides were sent blinded to an outside
142 laboratory of pathologists for anatomopathological analyses (Biodoxis Laboratories,
143 Romainville, France). Glomerular damage was defined by the presence of glomerulosclerosis
144 and glomerular cystic dilatation, whereas tubular lesions were defined by the following: (1)
145 necrosis; (2) regeneration and dilatation of the tubules; (3) interstitial inflammation; and (4)
146 fibrosis. The different types of lesions were scored from 0 to 4 for each animal. The total sum
147 of the scores of all lesions corresponded to the global score, and the percentage of each lesion
148 among the tubulointerstitial lesions was then calculated as previously described [28, 52].
149 Paraffin-embedded slices were deparaffinized and hydrated in descending gradations of ethanol
150 and in 3% H_2O_2 diluted in PBS to block endogenous peroxidase activity. For kidney injury
151 molecule-1 (KIM-1) staining, antigen retrieval was achieved with citrate buffer at pH=6.
152 Sections were then incubated overnight with anti-KIM-1 (Abcam, Paris, France, ab47635) at a
153 200-fold dilution at 4°C in a moist chamber. After washing, the slices were incubated with an
154 Alexa Fluor-conjugated goat anti-rabbit secondary antibody (1/1 000, Abcam, ab150061).
155 Finally, the nuclei were stained with Vectashield antifade mounting medium containing DAPI
156 for fluorescence visualization. Ten photomicrographs per animal were collected with a LEICA
157 DM 4000B fluorescence microscope, and semiquantification of fluorescent labeling was
158 performed with Histolab Software (version 8.12, Microvision Instruments, Lisses, France). For
159 intercellular adhesion molecule and vascular cell adhesion molecule (VCAM) staining, antigen
160 retrieval was achieved with Tris/EDTA buffer at pH=9. Sections were then incubated for 1 hour
161 with anti-ICAM-1 (Abcam, ab119871) diluted 250-fold or with anti-VCAM-1 (Abcam,
162 ab134047) diluted 1000-fold at room temperature in a moist chamber. After washing, the slices

were incubated with anti-rat and anti-rabbit secondary antibodies and finally developed using a DAB revelation kit (MMFrance, Brignais, France). Counterstaining with hematoxylin was performed to identify renal structures. For Microtubule-associated protein 1A/1B-light chain 3B (LC3-II) and Endoribonuclease/protein kinase IRE1-like protein (IRE1-α), antigen retrieval was achieved respectively with Tris/EDTA buffer at pH=9 or citrate buffer at pH=6. Sections were then incubated respectively for 1 or 2 hours with anti-LC3-II (Abcam, ab192890) diluted 1500-fold or with anti-IRE-1α (Novus Biologicals, NB100-2323) diluted 250-fold at room temperature in a moist chamber. After washing, the slices were incubated with an Alexa Fluor-conjugated goat anti-rabbit secondary antibody (1/1 000, Abcam, ab150061). Finally, the nuclei were stained with Vectashield antifade mounting medium containing DAPI for fluorescence visualization. Ten photomicrographs per animal were collected with a LEICA DM 4000B fluorescence microscope.

2.6. KIM-1 and CLU detection in the urine

KIM-1 and clusterin (CLU) were measured in urine samples using ELISA kits according to the manufacturer's instructions (R&D Systems, Lille, France). To comply with the concentration intervals of the assay, the urine samples were diluted 1:100 for the CLU assay and 1:10 to 1:100 for the KIM-1 assay.

2.7. Real-time RT-PCR

Total RNA was extracted from the renal cortex, dissected under binocular microscope, by following the manufacturer's instructions (Total RNA Isolation Kit, Qiagen, Les Ulis,France) and was reverse-transcribed into cDNA with a High-capacity cDNA Reverse Transcription Kit (Applied Biosystems Life Technologies, Courtabœuf, France). Real-time polymerase chain reactions (RT-PCR) was performed using two methods, namely, SYBR Green and Taqman, with 10 µL of 1 ng/µL cDNA per well and 2.5% v/v primers (Fisher Scientific, Illkirch, France), 83% v/v SYBR Green (Fisher Scientific, Illkirch, France), and 14.5% v/v sterile water. Table

188 1 shows the accession number and primer sequences of each gene used in this study for the
189 SYBR Green method, whereas Table 2 shows the accession number of the Taqman genes used
190 to analyze the mRNA levels of proteins involved in nephrotoxicity, inflammation, apoptosis,
191 autophagy and the unfolded protein response (UPR). QuantStudio 12K Flex (Applied
192 Biosystems Life Technologies, Courtabœuf, France) was used to detect the real-time RT-PCR
193 products. The comparative ΔΔCt method was used to determine the relative quantification of
194 each gene expression in comparison with the geometric average of the Ct values of the
195 housekeeping genes β-actin (ACTB), hypoxanthine-guanine phosphoribosyltransferase
196 (HPRT) and glyceraldehyde-3-phosphate dehydrogenase (GAPDH). Finally, the fold induction
197 for each treated group was calculated relative to the control group (NaCl).

198 **Table 1.**Primer sequences of the genes analyzed by real-time RT-PCR with SYBR Green.

Gene	Accession Number	Forward	Reverse
BAX	NM_007527	CCCCCCGAGAGGTCTTCTT	GCGGCCCCAGTTGAAGT
BCL2	NM_009741	TGGGATGCCTTTGTGGAACT	CAGAGACAGCCAGGAGAAATCAA
CASP3	NM_001284409	CTGGACTGTGGCATTGAGACA	GCCTCCACCGGTATCTTCTG
CLU	AF182509	TCGGGCATCTGGCATCA	AAGCTCACGGGCGAAGAAC
GAPDH	GU214026	TCCACTCACGGCAAATTCAACG	TAGACTCCACGACATACTCAGC
HPRT	NM_013556	TGCTGCGTCCCCAGACTTTTG	AGATAAGCGACAATCTACCAGAGG
ICAM-1	NM_010493	CACCCCAAGGACCCCAAGGAGAT	CGACGCCGCTCAGAAGAACCAC
KIM-1	BC053400	TTTCAGGCCTCATACTGCTTCTC	TGACCCACCACCCCCTTT
VCAM-1	BC029823	TCGCGGTCTTGGGAGCCTCA	TGACCGTGACCGGCTTCCCA

199

200 **Table 2.**Accession numbers of the Taqman genes used to analyze autophagy and the UPR.

Gene	Accession Number	Taqman gene reference
ACTB	NM_007393.5	Mm02619580_g1
HPRT	NM_013556.2	Mm03024075_m1
GAPDH	NM_001289726.1	Mm99999915_g1

AMPK	NM_001013367.3	Mm01296700_m1
ATF4	NM_001287180.1	Mm00515325_g1
ATF6	NM_001081304.1	Mm01295319_m1
BECLIN1	NM_019584.3	Mm01265461_m1
DRAM1	NM_027878.2	Mm00503627_m1
DRAM2	NM_001025582.2	Mm00509019_m1
GRP78	NM_001163434.1	Mm00517691_m1
GRP94	NM_011631.1	Mm00441926_m1
IRE1-A	NM_023913.2	Mm00470233_m1
LC3-II	NM_026160.4	Mm00782868_sH
PERK	NM_010121.2	Mm00438700_m1
SESTRIN2	NM_144907.1	Mm00460679_m1

2.8. Cellular viability and cellular death measurements

Pieces of the renal cortex (25 mg) were placed into 1.5 mL Eppendorf tubes with 250 µL hypotonic buffer containing 25 mM HEPES, 5 mM $MgCl_2$, 1 mM EDTA, 1 mM Pefabloc, 1 µg/mL pepstatin, 1 µg/mL leupeptin, and 1 µg/mL trypsin inhibitor. Then, the pieces were ground with micropestles and centrifuged at 13,000 rpm for 15 min at 4°C. The supernatants were collected and diluted 50-fold, and the protein concentrations of the supernatants were determined by the Bradford test. Then, the concentrations of the samples were adjusted to 1 mg/mL before the determination of cellular viability, cytotoxicity and caspase activity with a detection kit (Promega "ApoTox-Glo™ Triplex Assay", Charbonnières-les-Bains, France, G6320). The cleavage of the peptide GF-AFC substrate generated a fluorescent signal, which was used to measure live-cell protease activity in the kidneys. Another fluorogenic peptide substrate, called bis-AAF-R110 substrate, was used to measure dead-cell protease activity released during the loss of the cellular membrane integrity. Caspase 3/7 activity was determined

by measuring the release of luciferin after the cleavage of the luminogenic DEVD-peptide substrate by caspases 3 and 7.

2.9. Statistical analyses

Statistical analyses were performed using SigmaPlot 11.0 software (Systat Software, Inc., Erkrath, Germany), except for the semiquantification of the immunostainings, for which Histolab Software (Microvision Instruments) was used as described previously [28]. One-way analysis of variance (ANOVA) was used to compare each group, and the Holm-Sidak method was applied for multiple comparisons. For the semiquantification of immunostainings, a general estimating equation (GEE) was calculated using R 3.4.4 (version 3.4.4, R Core Team, Boston, MA, USA) and RStudio software packages (version 1.1.423, RStudio Inc., Boston, MA, USA). The level of significance was set at $p< 0.05$.

3. Results

3.1. U and F measurements

U content was measured in the mouse kidneys, 72 hours after ip treatment (Figure 2), whereas F content was measured in the urine 24 hours after ip treatment (Figure 3). The basal content of U in the kidneys of negative controls was very low (9.3 ng/g of tissue ± 0.3), corresponding to previously described natural U concentrations [18, 28]. For all treated groups a significantly increased U content was observed ($p<0.001$), reaching a maximum of 8.70 ng/mg of tissue (Figure 2). The level of U in the kidneys did not differ between groups regardless of the dose of U in the drinking water (10 to 40 mg/L) and it was similar to the level measured in the positive control group.

F could only be measured in the urine, as the tissue content of F in the control and treated animals was too low to show any difference by potentiometry (data not shown) [28]. Urine was

239 collected during two 24-hour periods, one before ip injection and another immediately after.
240 Before acute ip treatment, only the F level of the 50 mg/L F group, with a concentration of
241 36.2 µg F/24h, was significantly increased compared to that of the control group ($p<0.05$) (data
242 not shown), whereas after ip treatment a significant dose-dependent increase of F in the urine
243 was observed (Figure 3). The negative control mice showed a basal level of 5.0 µg F/24 hours,
244 whereas the positive controls excreted 94.3 µg of F in the urine 24 hours after ip treatment. The
245 highest priming dose of 50 mg/L F induced an increase in F excretion (155.6 µg/24 hours ±
246 14.4) that was significantly different from that in the 15- and 30-mg/L F-exposed groups
247 ($p<0.001$ and $p<0.05$, respectively), confirming that the increases in these measurements were
248 dependent on the dose of F chronic exposure.

249 *3.2. Histopathological scoring in the kidney after U and F exposure*

250 Seventy-two hours after challenge, HES staining (Figure 4A) allowed us to determine
251 global scoring of damage induced in the kidney by U and F (Figure 4B). In addition, the extent
252 of these damages (hyaline cast appearance, tubular vacuolization, necrosis and regeneration)
253 was quantified for each experimental group (Figure 4C) as previously done in our studies [28,
254 52].

255 The extent of renal lesion was detected in a limited number of animals, and there was no
256 significant increase between the scores of the exposed and control groups (Figure 4B). All
257 animals in the negative control group showed tubular vacuolization in their kidneys, but with
258 low severity ($p>0.05$). Global scores were increased after U exposure, but not significantly,
259 probably because of the basal damage in the negative control animals. However, U significantly
260 induced the formation of hyaline casts, tubular vacuolization and necrosis in all treated animals
261 compared to the negative control animals ($p<0.005$ for hyaline casts in 10 mg/L U-treated
262 animals, and $p<0.001$ for all other lesions) (Figure 4C). Non-exposed animals presented tubular
263 vacuolization, whereas hyaline cast formation and tubular necrosis were specifically induced

after U exposure. However, no significant differences between pre-exposed animals and positive control animals were observed under our experimental conditions, and no significant differences were observed between the groups of animals exposed to U or F through drinking water. The HES scores of the F groups were similar but lower. Nevertheless, hyaline cast formation, tubular regeneration and necrosis appeared in some animals exposed to F.

The histopathologic analysis revealed that neither U nor F induced glomerular damage in the kidneys.

3.3. Biomarkers of U- and F-induced nephrotoxicity: KIM-1 and CLU mRNA, urinary secretion and in situ *detection*

CLU and KIM-1 are proteins considered early biomarkers for a wide variety of acute and chronic renal impairments [53-56].

As shown in Figure 5A, the gene expression of KIM-1 was 3.7- and 1.8-fold increased by U and F challenge treatment, respectively ($p<0.05$). Similarly, the gene expression of CLU was induced in the kidneys by acute treatment with U, increasing 2.8-fold ($p<0.005$) (Figure 5B), but not after F acute exposure. Interestingly, for both U and F, all groups exposed to the priming doses through drinking water, except for the 20 mg/L U and the 50 mg/L F prime-exposed groups, had significantly induced KIM-1 and CLU gene expression. Indeed, the KIM-1 and CLU expression levels were not significantly different from those of the negative control group at these concentrations, indicating a possible decrease in nephrotoxicity and a potential adaptive response to these doses.

When looking at the urinary secretion of these proteins in Figures 5C and 5D, we can see that the levels of both proteins were significantly augmented in the urine of animals from the positive F control group, showing 4.8- and 2.1-fold increases in KIM-1 and CLU, respectively. Interestingly, the groups previously exposed to 15 and 30 mg/L F and then challenged with 7.5 mg/kg F injection, but not the group exposed to the priming dose of 50 mg/L, exhibited

289 increased urinary secretion of KIM-1 and CLU. Indeed, under these conditions (50 mg/L + 7.5
290 mg/kg), the KIM-1 and CLU urinary levels were not significantly different than those of the
291 negative control group. Their urinary levels were also significantly lower than those of the
292 positive control group (0 mg/L + 7.5 mg/kg) ($p<0.05$), confirming the hypothesis of reduced
293 nephrotoxicity and a potential adaptive response after pre-exposure to 50 mg/L F. In the case
294 of U, treatment with the challenge dose alone did not induce KIM-1 or CLU 24 hours after ip
295 injection. On the other hand, a priming exposure to 10 or 20 mg/L U induced 1.5- and 1.8-fold
296 decreases, respectively, in the basal level of CLU secretion in the urine ($p<0.05$ and $p<0.005$).
297 These differences between urinary and mRNA levels could be explained by the difference in
298 the timing of the analysis (24 and 72 hours after ip injection) and suggested that U-induced
299 nephrotoxicity cannot be detected 24 hours after ip treatment but can only be detected after a
300 longer period (48 or 72 hours).

301 The *in situ* detection of KIM-1 is shown in Figure 6. This protein was detected in the
302 proximal tubules of some control animals, revealing a basal level of renal impairment, and in
303 all U- and F-exposed mice (Figures 6A and 6C). In the group exposed to 50 mg/L F, only a few
304 animals showed *in situ* KIM-1 expression in the kidneys. *In situ* KIM-1 expression was
305 analyzed relative to that in the control group (fixed at 1.0), and the analysis revealed that acute
306 treatment with U alone significantly induced a 5.1-fold increase in protein expression in the
307 kidneys ($p<0.05$), whereas F did not, as shown in Figures 6B and 6D. A significant increase in
308 KIM-1 was detected in all groups that underwent priming exposure to U ($p<0.001$), except those
309 that were exposed to a dose of 10 mg/L. For F, *in situ* KIM-1 expression in the kidneys was not
310 significantly induced in any group, even though increasing tendencies, specifically 4.2- and 3.1-
311 fold increases were observed in mice contaminated with 15 and 30 mg/L F, respectively before
312 challenge. Interestingly, chronic priming exposure to 50 mg/L F led to a level of KIM-1 that
313 appeared to be lower than the level in negative controls (50% of the basal expression).

Nevertheless, these results are in accordance with the gene expression of KIM-1 and its urinary secretion and consolidate the hypothesis of an adaptive response for the group exposed to a priming concentration of 50 mg/L F.

3.4. Gene expression of factors involved in the potential adaptive mechanisms of U and F

The mRNA expression of the genes shown in Figure 7 allows us to approvide general guidance on the mechanisms potentially implicated in the renal adaptive response to U and F. The fold induction of each group was calculated relative to the control group which was fixed at an mRNA level of 1.0 (group not shown in the figure).

ICAM and VCAM are both proteins involved in the recruitment of inflammatory cells and therefore are good markers of the potential inflammation induced by U and F. The mRNA level of ICAM was not induced in positive controls, whereas it was induced 1.9- and 2.0-fold in the kidney of mice that received the priming doses of 10 and 40 mg/L U ($p<0.005$ and $p<0.001$, respectively). The overexpression of VCAM was slightly induced in animals from the positive control group and the group pre-exposed to 10 mg/L, ($p<0.05$). No induction of either ICAM or VCAM was observed at the priming concentration of 20 mg/L, suggesting that no inflammation was induced at this concentration (Figure 7A). In contrast, no induction of either ICAM or VCAM mRNA expression was observed after F exposure under our conditions (Figure 7B).

Bax and BCl2 are known to be pro- and anti-apoptotic proteins, whereas the gene Casp-3 encodes the effector apoptotic protein caspase 3. Under our conditions, all groups of mice that received the challenge dose of U showed a slightly increased expression of the anti-apoptotic protein BCl2, not exceeding a 1.4-fold increase ($p<0.05$ to $p<0.001$) (Figure 7A). In contrast, the gene expression of the pro-apoptotic protein Bax was increased only after a priming exposure to 10 mg/L U ($p<0.005$), but showed a low 1.2-fold increase. No induction of Casp-3 was observed after U exposure under our conditions. In contrast with the induction observed

339 with U, no induction of BCl2, Bax or Casp-2 gene expression was induced with the challenge
340 dose of F (Figure 7B). However, a slight 1.2-fold induction of BCl2 mRNA was observed in
341 all groups of mice exposed to the priming concentrations of F ($p<0.05$), whereas the gene
342 expression of Bax was increased only after a priming exposure to 15 mg/L F ($p<0.05$). Bax and
343 Casp-3 gene expression was significantly reduced compared to that in the positive control group
344 after a priming exposure to 30 mg/L F.

345 Beclin1 and LC3-II are both genes coding for proteins involved in autophagy, whereas
346 Sestrin2, AMPK and DRAMs are genes known to be induced by autophagy. In the case of U,
347 as shown in Figure 7A, the gene expression of AMPK was slightly increased (1.2-fold increase)
348 in positive controls ($p<0.005$), whereas the same treatment significantly reduced the gene
349 expression of DRAM2 ($p<0.001$). Mice previously contaminated with the priming doses of U
350 also showed increased mRNA levels of AMPK but showed a low 1.3-fold induction ($p<0.001$).
351 Interestingly, the groups that received the priming doses of 20 and 40 mg/L presented
352 significantly higher AMPK gene expression than that presented by the positive control group
353 ($p<0.05$). In contrast, all groups exposed to the priming doses of U showed significantly reduced
354 gene expression of DRAM2 ($p<0.001$), similar to the positive control group, whereas the
355 priming dose of 10 mg/L U increased the mRNA expression of DRAM1 ($p<0.005$). At the same
356 priming dose of 10 mg/L U, mice presented a small increase in the mRNA expression of LC3-
357 II ($p<0.05$), a protein known to be involved in autophagosome formation and therefore in the
358 last step of autophagy. As shown in Figure 7B, the F challenge dose did not induce any of the
359 genes implicated in autophagy we investigated. However, F induced DRAM2 gene expression
360 in the group exposed to 50 mg/L and then treated with the challenge dose of 7.5 mg/kg NaF
361 when compared to the negative and positive controls ($p<0.05$ and $p<0.005$, respectively).
362 Moreover, at the priming dose of 30 mg/L F the mRNA expression of SESTRIN2 was

363 significantly decreased compared to that in the negative and positive control groups ($p<0.001$
364 and $p<0.05$, respectively).

365 PERK, ATF6, IRE1-α, and ATF4 are involved in the three pathways of the UPR and
366 GRP78 and GRP94 are both genes induced by this biological response. Interestingly, ATF4
367 gene expression was induced in all groups treated with U (Figure 7A) regardless of whether
368 they experienced a priming exposure before being challenged ($p<0.001$). Nevertheless, only the
369 animals pre-exposed to 10 and 20 mg/L U showed an increased IRE1-α mRNA level compared
370 to that in the negative control group ($p<0.05$), and GRP78 gene expression was also increased
371 after the priming exposure of 10 mg/L followed by the challenge dose ($p<0.05$). In contrast,
372 there was no induction of the genes involved in the UPR after F treatment, as shown in Figure
373 7B.

374 In summary, Figures 7A and 7B show that U challenge treatment induced the expression
375 of genes involved in inflammatory cell recruitment, apoptosis, autophagy and the UPR, whereas
376 none of these genes were induced after F challenge in mice. It seems that U priming exposure
377 slightly induced genes involved in all these mechanisms, whereas only genes implicated in
378 apoptosis and autophagy were slightly modulated by F priming exposure. To further explore
379 the implication of these mechanisms, we observed specific markers, through enzymatic activity
380 measurements and *in situ* immunochemistry.

381 *3.5.* In situ *ICAM-1 and VCAM-1 expression in the kidney*

382 To determine whether either U or F can induce the recruitment of inflammatory cells in the
383 kidney, the quantification of *in situ* ICAM-1 and VCAM-1 expression was performed. A basal
384 level of CAM proteins was detected (Figure 8A and 8B), and *in situ* ICAM and VCAM
385 expression was quantified relative to that in the negative control group (fixed at 1.0). Mice did
386 not show any significant induction of ICAM-1 in the kidney after U challenge treatment (Figure
387 8C), but U did induce VCAM-1 expression in the kidney of mice challenged with 5 mg/kg,

388 regardless of whether they received priming exposure ($p<0.05$) (Figure 8D). It seems that a
389 priming exposure to 20 mg/L U induced the level of ICAM-1 significantly, eliciting a 1.5-fold
390 induction compared to that in the control group ($p<0.05$). When challenged with F, mice did
391 not show any significant induction of ICAM-1 in the kidney (Figure 8C) but showed a 1.4–fold
392 induction of *in situ* VCAM-1 expression ($p<0.05$) (Figure 8D). A priming exposure to 30 mg/L
393 F followed by a challenge injection of F, induced the *in situ* level of ICAM-1 significantly,
394 eliciting a 2.2-fold induction compared to that in the negative control group ($p<0.005$). On the
395 other hand, the groups exposed to the priming doses of 30 and 50 mg/L F showed significantly
396 lower expression levels of VCAM-1 compared to those in the positive control group ($p<0.001$
397 and $p<0.005$, respectively) but did not show any significant difference compared to the
398 nonexposed animals.

399 *3.6. Viability and cell death measurements in the kidneys*

400 Cell viability and death were studied by measuring enzymatic activities in tissue
401 homogenates prepared from the renal cortex (Figure 9). A challenge treatment of 5 mg/kg U
402 induced cytotoxicity and apoptosis to 155% and 122% of the control basal level, respectively
403 ($p<0.05$). Under our conditions, priming exposure to 10 or 20 mg/L U abolished the cytotoxicity
404 induced by the U challenge dose alone. Moreover, contamination with 20 mg/L U through
405 drinking water also abolished the apoptosis induced challenge with ip U injection. Indeed, this
406 group did not present significant differences compared with the negative control group, and its
407 caspase 3/7 activity was significantly lower than that of the positive control group ($p<0.001$).
408 All F-treated groups, except for the 15 mg/L F pre-exposed mice, which presented a small
409 decrease in caspase 3/7 activity to 87% of the basal level, presented similar rates of cell viability
410 and death compared to those in the negative control group ($p<0.05$). In conclusion, F did not
411 modulate cell viability or death at our working concentrations, but a renal adaptive response to
412 cytotoxicity and apoptosis induced by chronic exposure to 20 mg/L U in mice was suggested.

3.6. In situ *LC3-II measurement in the kidneys and the induction of autophagy*

LC3-II is the form of microtubule-associated protein 1A/1B-light chain 3 (LC3), that is conjugated to phosphatidylethanolamine and recruited to the autophagosomal membranes [57]. Therefore, the induction of autophagy in kidney cells has been studied through the immunodetection of the LC3-II protein *in situ* (Figure 10).

In negative control animals, no LC3-II was detected, as shown in Figure 10A. U induced LC3-II in the kidneys of challenged mice regardless of whether the animals were pre-exposed to priming doses of U, with scores ranging from 1.6 to 2.3 ($p<0.001$) (Figures 10A and 10B). Indeed, the scattered staining observed in the positive control and 10 mg/L U and 20 mg/L U-pre-exposed groups, indicated the formation of LC3-II from the cytosolic protein LC3-I, whereas LC3-II puncta, particularly noticeable in the magnified image of a 40 mg/L U-pre-exposed mouse, indicated the recruitment of the protein to the autophagosomal membranes. In addition, regardless of the type of exposure (challenged animals with or without priming exposures), F did not induce *in situ* LC3-II expression.

3.7. In situ *IRE1-α measurement in the kidneys and the induction of the UPR*

The IRE1-α protein is mainly involved in one of the three known pathways of UPR induction. Therefore, its overexpression in the cell cytosol was a good marker for the study of UPR induction after contamination.

In the negative groups, there was a basal level of tubule staining (approximately 24-30 %), as observed in Figure 11A. Animals challenged with U showed a significant increase in *in situ* IRE1-α expression compared to that in the negative control group ($p<0.05$), as the animals previously exposed to priming doses of U showed a staining rate of tubules up to 35% ($p<0.001$) (Figure 11B). The F positive control group showed the induction of IRE1-α *in situ* compared to that in the negative control group ($p<0.001$) (Figure 11C), similar to the priming exposed groups to 15, 30 and 50 mg/L ($p<0.005$, $p<0.001$ and $p<0.001$, respectively). Interestingly, the

438 animals exposed to 50 mg/L F through drinking water presented overexpression of the *in situ*
439 protein compared to that in the group pre-exposed to 15 mg/L ($p<0.05$). Moreover, this group
440 presented a higher expression of IRE1-α than the positive control group, but this difference was
441 not statistically significant ($p=0.068$).

442 **4. Discussion**

443 The adaptive response is a process that can occur at exposures to low doses of chemicals
444 or radiation stress [47, 49, 58]. The most frequently described protocol for inducing the adaptive
445 response is challenge following a previous priming exposure to a low dose [38, 48, 59]. It is
446 known that U and F are both nephrotoxic after acute exposures [15, 28-32, 50, 60, 61], but
447 previous studies including ours have shown that U and F may trigger a renal adaptive response
448 after chronic low-dose exposures [18, 37, 38, 44, 62]. This work allowed us to identify the
449 mechanisms of this adaptive response to exposures to chronic low doses of U and F through a
450 chronic priming chronic exposure to low doses of U or F followed by challenge treatment
451 delivered acutely and at nephrotoxic doses to mice. The challenge dose was previously selected
452 from our recent study of U and F acute treatments [28].

453 In this study, we have shown that the adaptive response is induced after priming exposure
454 to 20 mg/L for U and 50 mg/L for F. A pre-exposure to 20 mg/L U decreased the overexpression
455 of CLU and KIM-1 mRNA triggered by the challenge dose of 5 mg/kg U without inducing any
456 difference relative to the negative control (Figures 5A and 5B). On the other hand, U induced
457 *in situ* KIM-1 expression in all groups (challenge or prime + challenge) except in the 10 mg/L
458 U-pre-exposed group. Thus, the renal adaptive response to U observed under our conditions
459 mainly occurred at a dose of 20 mg/L. Our previous studies performed in rodents showed that
460 a 9-month exposure to 40 mg/L U does not induce renal histopathological lesions, nephrotoxic
461 biomarkers [39, 52], or glomerular filtration rate changes [18, 63]. Moreover, renoprotective
462 mechanisms such as the induction of glutathione are induced dose-dependently [18]. Previous

studies have shown that UN is not nephrotoxic when delivered chronically to rodents at concentrations ranging from 1 to 600 mg/L UN [18, 39, 52, 63], despite one study showing the appearance of tubular lesions without dose-dependent increases in severity, after a 28- or 91-day exposure to doses ranging from 0.96 to 600 mg/L [36]. The renal adaptive response triggered by U in drinking water has not yet been identified, but it was previously described that U is able to induce a renoprotective response *in vivo* after a single acute subtoxic dose of UN [38, 62]. Our study is the first to clearly demonstrate that U induces a renal adaptive response *in vivo* after chronic exposure to low doses of U in drinking water. Analyses of both the mRNA levels and the urinary protein secretion of CLU and KIM-1 revealed an adaptive response to F at 50 mg/L (Figure 5). Indeed, the KIM-1 and CLU levels in this group were not significantly different from those in the negative control group, whereas the mRNA expression and urinary secretion of these proteins were significantly decreased compared to those in the positive control group. Interestingly, chronic exposure to 50 mg/L F for 40 days induces nephrotoxic biomarkers such as the KIM-1, CLU or OPN genes and urinary protein levels in rats [40], but a 60-day period of exposure does not induce any histological damage [64]. However, rats treated with a priming exposure of the same dose before nephrotoxic treatment with gentamicin, compared to animals treated with gentamicin only, exhibit a decrease in F-induced nephrotoxicity, gene expression and protein secretion of KIM-1 and CLU [44]. Our findings are in accordance with this study and confirm the adaptive response observed at 50 mg/L F.

The mechanisms involved in this adaptive response have been studied to attain a better comprehension of the toxicological effects of low-dose exposure to U or F. Several mechanisms have been described in the literature as being involved in the adaptive response to chemicals or irradiation [49]. Among them, apoptosis, autophagy, the inflammatory response and the UPR have been reported to be induced by U and F [40, 44, 65-68] and could be involved in the U

488 and F adaptive response. It was previously shown that autophagy is able to reduce the toxic
489 effects induced by U in organs other than the kidneys [66, 69] and those induced by other
490 chemicals in the kidneys [70]. However, to our knowledge, we are the first to demonstrate that
491 autophagy is induced by U in the kidneys, *in vivo*. Indeed, through gene expression analysis
492 (Figure 7), we observed that the 20 mg/L U and 40 mg/L U-treated groups showed an adaptive
493 increase in AMPK gene expression and that the priming dose of 10 mg/L induced LC3-II and
494 DRAM1, genes known to be induced by autophagy. Moreover, animals pre-exposed to 10 and
495 20 mg/L U had an increased IRE1-α mRNA level, whereas the challenge dose alone did not
496 induce IRE1-α gene expression. Interestingly, our results showed the induction of autophagy
497 and the UPR after U challenge, regardless of whether there was a priming exposure (Figures 10
498 and 11). The UPR was also induced by F in the positive control group, as in the animals that
499 received the priming doses. This was the first study to show that U or F induces the UPR in the
500 kidneys *in vivo*. Nevertheless, our results do not identify autophagy and the UPR as mechanisms
501 involved in the adaptive response observed under our conditions. However, we cannot exclude
502 these mechanisms, as it is possible that autophagy and/or the UPR are induced during priming
503 exposure or after a recovery period between the priming and challenge doses. Further studies
504 will be necessary to investigate the induction of these mechanisms at other periods of exposure
505 at similar doses.

506 The gene expression analysis shown in Figure 7 indicates that inflammation and the
507 modulation of CAM mRNA expression could be mechanisms involved in the adaptive response
508 to U and F. Interestingly, in the case of F, *in situ* VCAM-1 levels were induced in the kidneys
509 by the challenge dose alone but not when mice were exposed to the priming doses of 30 and 50
510 mg/L F. This decrease in *in situ* VCAM-1 expression could partly explain the adaptive response
511 to F observed at 50 mg/L, under our conditions. As ICAM-1 is overexpressed in the kidneys of
512 animals pre-exposed to 30 mg/L F, the potential recruitment of inflammatory cells in the group

513 of mice that received this priming exposure needs further investigation (Figure 8A). It has been
514 shown that inflammation is modulated in the intestine after the chronic ingestion of U in rodents
515 [63, 71], but our results showed that U induced VCAM-1 in the kidneys of challenged mice
516 (Figure 8B) regardless of whether the mice received priming exposures. Therefore, similar to
517 autophagy and the UPR, the modulation of inflammatory cell recruitment cannot be identified
518 as a mechanism of the adaptive response to U.

519 Apoptosis, another mechanism studied, was identified as a mechanism involved in adaptive
520 response to U under our conditions, whereas no changes were observed after F exposures
521 (Figure 9). Indeed, both groups of animals with priming exposures to 20 and 40 mg/L U had
522 similar caspase 3/7 levels as those of the negative control group. Moreover, a priming exposure
523 to 20 mg/L U significantly reduced the caspase 3/7 activity induced by the challenge dose alone,
524 showing that apoptosis is at least partly involved in the adaptive response to U. In comparison,
525 other metals such as cadmium have been shown to reduce oxidative stress and induce less
526 apoptosis after chronic exposure compared to acute exposure [72, 73]. In contrast, apoptosis
527 and autophagy are induced in mouse hepatocytes after chronic exposure to 50 mg/L NaF for
528 150 days [74]; this difference can be explained by a tissue-specific response or the duration of
529 the exposure.

530 Our data demonstrate the existence of a renal adaptive response to chronic exposure to low
531 doses of U and F involving the induction of adaptive mechanisms including apoptosis and
532 inflammatory regulation in mice. Our results allowed us to identify molecular targets partly
533 responsible for these adaptive mechanisms: downregulation of the activities of the effector
534 caspases 3/7 and a decrease in *in situ* VCAM expression. Moreover, KIM-1 protein is
535 cytoprotective because of its role in the phagocytosis of cellular debris produced by the
536 apoptosis of tubular cells [75, 76] and its overexpression in our study may have been
537 cytoprotective and played a role in the adaptive response observed in the group pre-exposed to

20 mg/L U. Overall, these results allow a better understanding of the effects of chronic exposure to low doses of U and F on an organism and provide new knowledge for the (radio)protection of individuals. They raise the question of a higher or lower risk window - in certain ranges of doses where the adaptive response is induced - and of their applications in humans. Indeed, the use of fine and specific biomarkers of renal impairment in humans could allow better assessment of renal function during exposures to low doses of U or F.

Funding

This research did not receive any specific grant from funding agencies in the public, commercial, or not-for-profit sectors.

Acknowledgements

We would like to thank Mohamed Amine Benadjaoud (IRSN/PSE-SANTE/SERAMED) for his valuable advice on statistical analyses using R software. We also thank the animal care team (IRSN/PSE-SANTE/GSEA), including the zoological technicians Marine Gauthe, Romain Granger, Birame Mane, Amandine Sache, Frederic Voyer and Chrysostome Yiannakis and the veterinarian Delphine Denais-Lalieve.

Conflict of interest statement

The authors report no conflict of interest.

Figures captions

Figure 1. General scheme of the distribution of mice into uranium- and fluoride-treated groups (n=10-18 per group) and the doses administered.

Figure 2. Measurement of U in the kidneys of mice that drank contaminated water (0, 10, 20, 40 mg/L U) for 6 months and were acutely injected with 5 mg/kg U or NaCl (n=10-12 per group). The results are presented as the mean ± standard error of the mean. The asterisk represents a significant difference compared with the negative control group (*** $p<0.001$).

Figure 3. Measurement of F in the urine of mice that drank contaminated water (0, 15, 30, 50 mg/L F) for 6 months and were acutely injected with 7.5 mg/kg NaF or NaCl (n=11-18 per group). The results are presented as the mean ± standard error of the mean. The asterisk represents a significant difference compared with the negative control group (0 mg/L + 0 mg/kg), and the dollar symbol represents a significant difference compared with the positive control group (0 mg/L + 7.5 mg/kg). The number of symbols (1, 2, or 3) corresponds to the level of significance ($p<0.05$, $p<0.005$, and $p<0.001$).

Figure 4. Representative photomicrographs (**A**) (200x) of noticeable renal lesions after HES staining in control mice, U-contaminated (40 mg/L and 5 mg/kg U) mice and F-contaminated (30 mg/L F and 7.5 mg/kg NaF) mice. The letters G, PT, and HC indicate glomeruli, proximal tubules, and hyaline casts, respectively. Tubular vacuolization is indicated by black circles, whereas tubular necrosis is indicated by black rectangles. The renal lesion scores (**B**) are presented as the mean ± standard error of the mean (n=10-18 per group) were done blinded. The percentage of tubular and interstitial injuries (basophilic tubules, tubular necrosis, vacuolization and hyaline casts) in kidneys 72 hours after ip injection (**C**) is presented as the mean. The asterisk represents a significant difference compared with the negative control group (0 mg/L + 0 mg/kg) (two-way ANOVA with Holm-Sidak correction, *$p<0.05$, **$p<0.005$, and ***$p<0.001$).

Figure 5. Gene expression levels of the sensitive nephrotoxicity markers KIM-1 and CLU in the renal cortex 72 hours after ip injection (**A-B**) and their urinary protein levels directly after IP injection

582 [77]. Mice were chronically exposed for 6 months by drinking contaminated water (0, 10, 20, 40 mg/L
583 U or 0, 15, 30, 50 mg/L F) and then acutely injected with either NaCl, 5 mg/kg U or 7.5 mg/kg NaF.
584 The results are presented as the mean ± standard error of the mean (n=10-18 per group for mRNA and
585 n=10-12 for protein). The asterisk represents a significant difference compared with the negative control
586 group (0 mg/L + 0 mg/kg), and the dollar symbol represents a significant difference compared with the
587 positive control group (0 mg/L + 5 mg/kg for U and 0 mg/L + 7.5 mg/kg for F). The number of symbols
588 (1, 2, or 3) corresponds to the level of significance ($p<0.05$, $p<0.005$, and $p<0.001$).

589 **Figure 6.** Representative photomicrographs (200x) of the *in situ* renal expression of the protein
590 KIM-1 (in green) in mice chronically exposed for 6 months by drinking contaminated water (0, 10, 20,
591 40 mg/L U or 0, 15, 30, 50 mg/L F) and then acutely injected with either NaCl, 5 mg/kg U or 7.5 mg/kg
592 NaF (**A; C**) (n=10-18 per group). The results of the semiquantification of KIM-1 scoring (**B; D**) are
593 presented as the mean ± standard error of the mean (n=10-18 per group). The asterisk represents a
594 significant difference compared with the negative control group (0 mg/L + 0 mg/kg). The number of
595 symbols (1, 2, or 3) corresponds to the level of significance ($p<0.05$, $p<0.005$, and $p<0.001$) (general
596 estimating equation for normal regression).

597 **Figure 7.** Gene expression of molecules involved in inflammation (in orange), apoptosis (in green),
598 autophagy (in purple), and the UPR (in red) in the renal cortex 72 hours after the ip injection of mice
599 chronically exposed to U (**A**) and F (**B**). Mice were exposed for 6 months by drinking contaminated
600 water (0, 10, 20, 40 mg/L U or 0, 15, 30, 50 mg/L F) and then acutely injected with either NaCl, 5 mg/kg
601 U or 7.5 mg/kg NaF. The results are presented as the mean ± standard error of the mean relative to the
602 control group (n=10-18 per group). The asterisk represents a significant difference compared with the
603 negative control group (0 mg/L + 0 mg/kg), and the dollar symbol represents a significant difference
604 compared with the positive control group (0 mg/L + 5 mg/kg for U and 0 mg/L + 7.5 mg/kg for F). The
605 number of symbols (1, 2, or 3) corresponds to the level of significance ($p<0.05$, $p<0.005$, and $p<0.001$).

606 **Figure 8.** Representative photomicrographs (200x) of the *in situ* renal expression of the proteins
607 ICAM-1 (**A**) and VCAM-1 (**B**) in non-exposed and chronically exposed mice (0 and 30 mg/L F or 0 and

20 mg/L U) before challenge injection (0 and 7.5 mg/kg NaF or 0 and 5 mg/kg U). The results of the semiautomatic quantification of ICAM-1 (**C**) and VCAM-1 (**D**) are presented as the mean ± standard error of the mean (n=10-18 per group). The asterisk represents a significant difference compared with the negative control group (0 mg/L + 0 mg/kg), and the dollar symbol represents a significant difference compared with the positive control group (0 mg/L + 5 mg/kg for U and 0 mg/L + 7.5 mg/kg for F). The number of symbols (1, 2, or 3) corresponds to the level of significance ($p<0.05$, $p<0.005$, and $p<0.001$) (general estimating equation for normal regression).

Figure 9. Cell viability, cytotoxicity and caspase 3/7 activity in the renal cortex of mice 72 hours after ip U and F injections. Mice were chronically exposed for 6 months by drinking contaminated water (0, 10, 20, 40 mg/L U or 0, 15, 30, 50 mg/L F) and then acutely injected with either NaCl, 5 mg/kg U or 7.5 mg/kg NaF. The results are presented as the mean percentage relative to the negative control group ± standard error of the mean (n=10-18 per group). The asterisk represents a significant difference compared with the negative control group (0 mg/L + 0 mg/kg), and the dollar symbol represents a significant difference compared with the positive control group (0 mg/L + 5 mg/kg for U and 0 mg/L + 7.5 mg/kg for F). The number of symbols (1, 2, or 3) corresponds to the level of significance ($p<0.05$, $p<0.005$, and $p<0.001$).

Figure 10. Representative photomicrographs (400x) of the protein *in situ* renal expression of LC3-II (in green) in mice chronically exposed for 6 months, by drinking contaminated water (0, 10, 20, 40 mg/L U or 30 mg/L F) and then acutely injected with either NaCl, 5 mg/kg U or 7.5 mg/kg NaF (**A**) (n=10-12 per group). The results of the semiquantification of LC3B scoring after U exposure (**B**) are presented as the mean ± standard error of the mean. The asterisk represents a significant difference compared with the negative control group (0 mg/L + 0 mg/kg) (general estimating equation for normal regression, ***$p<0.001$). An enlarged image (**C**) after exposure to 40 mg/L and 5 mg/kg U to show the green puncta of LC3-II, which represent protein recruitment to autophagosome membranes, is presented.

Figure 11. Representative photomicrographs (200x) of the *in situ* renal expression of the protein IRE1-α (in green) in control mice and mice exposed over a 6-month period to either 50 mg/L F or 40

634 mg/L U in drinking water and then acutely injected with 7.5 mg/kg F or 5 mg/kg U, respectively (**A**)
635 (n=10-12 per group). The number of IRE1-α-positive tubules after U (**B**) or F exposure (**C**) is presented
636 as the mean ± standard error of the mean. The asterisk represents a significant difference compared with
637 the negative control group (0 mg/L + 0 mg/kg) (*p<0.05, **p<0.005, and ***p<0.001) (general
638 estimating equation for normal regression).

639

Bibliography

[1] M. Waziri, U. Musa, S.S. Hati, Assessment of fluoride concentrations in surface waters and groundwater sources in northeastern Nigeria, Resour Environ 2(2) (2012) 67-72.

[2] R. Juntunen, Etelä-Suomen kallioporakaivojen uraani-ja radontutkimukset (Uranium and radon in wells drilled into bedrocks in southern Finland), Report of Investigation, Geological Survey of Finland, Espoo 98 (1991).

[3] L. Salonen, 238U series radionuclides as a source of increased radioactivity in groundwater originating from Finnish bedrock, Future Groundwater Resources at Risk (Proceedings of the Helsinki Conference, June 1994) 222 (1994).

[4] O. Barbier, L. Arreola-Mendoza, L.M. Del Razo, Molecular mechanisms of fluoride toxicity, Chem Biol Interact 188(2) (2010) 319-33.

[5] WHO, Fluoride in drinking-water, Switzerland, 2006.

[6] WHO, Guidelines for drinking-water Quality, World Health Organization, Geneva, Switzerland, 2011.

[7] D. Browne, H. Whelton, D. O'Mullane, Fluoride metabolism and fluorosis, Journal of dentistry 33(3) (2005) 177-86.

[8] Y. Guéguen, L. Roy, S. Hornhardt, C. Badie, J. Hall, S. Baatout, E. Pernot, L. Tomasek, O. Laurent, T. Ebrahimian, C. Ibanez, S. Grison, S. Kabacik, D. Laurier, M. Gomolka, Biomarkers for uranium risk assessment for the development of the CURE (Concerted Uranium Research in Europe) molecular epidemiological protocol, Radiation Research 187(1) (2017) 107-127.

[9] UNSCEAR, Sources, effects and risks of ionizing radiation, United Nations Scientific Committee on the Effects of Atomic Radiation, U.S., 2016.

[10] X. Xiong, J. Liu, W. He, T. Xia, P. He, X. Chen, K. Yang, A. Wang, Dose-effect relationship between drinking water fluoride levels and damage to liver and kidney functions in children, Environ Res 103(1) (2007) 112-6.

[11] Y.D. La Touche, D.L. Willis, O.I. Dawydiak, Absorption and biokinetics of U in rats following an oral administration of uranyl nitrate solution, Health physics 53(2) (1987) 147-62.

[12] E. Craft, A. Abu-Qare, M. Flaherty, M. Garofolo, H. Rincavage, M. Abou-Donia, Depleted and natural uranium: chemistry and toxicological effects, Journal of toxicology and environmental health. Part B, Critical reviews 7(4) (2004) 297-317.

[13] L. Vicente-Vicente, Y. Quiros, F. Perez-Barriocanal, J.M. Lopez-Novoa, F.J. Lopez-Hernandez, A.I. Morales, Nephrotoxicity of uranium: pathophysiological, diagnostic and therapeutic perspectives, Toxicological sciences : an official journal of the Society of Toxicology 118(2) (2010) 324-47.

[14] S.A. Katz, The Chemistry and Toxicology of Depleted Uranium Toxics 2(1) (2014) 50-78.

[15] T. Dote, K. Kono, K. Usuda, H. Nishiura, T. Tagawa, Acute renal damage dose response in rats to intravenous infusion of sodium fluoride, Fluoride 33(4) (2000) 210-217.

[16] S.L. Manocha, H. Warner, Z.L. Olkowski, Cytochemical response of kidney, liver and nervous system of fluoride ions in drinking water, The Histochemical journal 7(4) (1975) 343-55.

[17] F. Paquet, P. Houpert, E. Blanchardon, O. Delissen, C. Maubert, B. Dhieux, A.M. Moreels, S. Frelon, P. Gourmelon, Accumulation and distribution of uranium in rats after chronic exposure by ingestion, Health physics 90(2) (2006) 139-47.

[18] C. Poisson, J. Stefani, L. Manens, O. Delissen, D. Suhard, C. Tessier, I. Dublineau, Y. Gueguen, Chronic uranium exposure dose-dependently induces glutathione in rats without any nephrotoxicity, Free radical research 48(10) (2014) 1218-31.

[19] K. Usuda, K. Kono, T. Dote, K. Nishiura, K. Miyata, H. Nishiura, M. Shimahara, K. Sugimoto, Urinary biomarkers monitoring for experimental fluoride nephrotoxicity, Arch Toxicol 72(2) (1998) 104-9.

[20] M.L. Zamora, J.M. Zielinski, G.B. Moodie, R.A. Falcomer, W.C. Hunt, K. Capello, Uranium in drinking water: renal effects of long-term ingestion by an aboriginal community, Archives of environmental & occupational health 64(4) (2009) 228-41.

690 [21] M.L. Zamora, B.L. Tracy, J.M. Zielinski, D.P. Meyerhof, M.A. Moss, Chronic ingestion of uranium in
691 drinking water: a study of kidney bioeffects in humans, Toxicological sciences : an official journal of the
692 Society of Toxicology 43(1) (1998) 68-77.
693 [22] H.M. Wasana, D. Aluthpatabendi, W.M. Kularatne, P. Wijekoon, R. Weerasooriya, J. Bandara,
694 Drinking water quality and chronic kidney disease of unknown etiology (CKDu): synergic effects of
695 fluoride, cadmium and hardness of water, Environmental geochemistry and health 38(1) (2016) 157-
696 68.
697 [23] O. Lantz, M.H. Jouvin, M.C. De Vernejoul, P. Druet, Fluoride-induced chronic renal failure,
698 American journal of kidney diseases : the official journal of the National Kidney Foundation 10(2)
699 (1987) 136-9.
700 [24] P. Kurttio, A. Harmoinen, H. Saha, L. Salonen, Z. Karpas, H. Komulainen, A. Auvinen, Kidney toxicity
701 of ingested uranium from drinking water, American journal of kidney diseases : the official journal of
702 the National Kidney Foundation 47(6) (2006) 972-82.
703 [25] P. Kurttio, A. Auvinen, L. Salonen, H. Saha, J. Pekkanen, I. Makelainen, S.B. Vaisanen, I.M. Penttila,
704 H. Komulainen, Renal effects of uranium in drinking water, Environ Health Perspect 110(4) (2002) 337-
705 42.
706 [26] M.I. Jimenez-Cordova, M. Cardenas-Gonzalez, G. Aguilar-Madrid, L.C. Sanchez-Pena, A. Barrera-
707 Hernandez, I.A. Dominguez-Guerrero, C. Gonzalez-Horta, O.C. Barbier, L.M. Del Razo, Evaluation of
708 kidney injury biomarkers in an adult Mexican population environmentally exposed to fluoride and low
709 arsenic levels, Toxicology and applied pharmacology 352 (2018) 97-106.
710 [27] K.B. Jayasekara, D.M. Dissanayake, R. Sivakanesan, A. Ranasinghe, R.H. Karunarathna, G.W.
711 Priyantha Kumara, Epidemiology of chronic kidney disease, with special emphasis on chronic kidney
712 disease of uncertain etiology, in the north central region of Sri Lanka, Journal of epidemiology 25(4)
713 (2015) 275-80.
714 [28] A. Bontemps, L. Conquet, C. Elie, V. Magneron, C. Gloaguen, D. Kereselidze, K. Tack, O.C. Barbier,
715 Y. Gueguen, In Vivo Comparison of the Phenotypic Aspects and Molecular Mechanisms of Two
716 Nephrotoxic Agents, Sodium Fluoride and Uranyl Nitrate, International journal of environmental
717 research and public health 16(7) (2019).
718 [29] T. Dote, K. Kono, K. Usuda, H. Nishiura, T. Tagawa, K. Miyata, M. Shimahara, N. Hashiguchi, J.
719 Senda, Y. Tanaka, Toxicokinetics of intravenous fluoride in rats with renal damage caused by high-dose
720 fluoride exposure, International archives of occupational and environmental health 73 Suppl (2000)
721 S90-2.
722 [30] P. Sangeetha Vijayan, P.D. Rekha, U. Dinesh, A.B. Arun, Biochemical and histopathological
723 responses of the Swiss albino mice treated with uranyl nitrate and its recovery, Renal failure 38(5)
724 (2016) 770-5.
725 [31] M.P. Santoyo-Sanchez, M. del Carmen Silva-Lucero, L. Arreola-Mendoza, O.C. Barbier, Effects of
726 acute sodium fluoride exposure on kidney function, water homeostasis, and renal handling of calcium
727 and inorganic phosphate, Biological trace element research 152(3) (2013) 367-72.
728 [32] J.M. Taylor, J.K. Scott, E.A. Maynard, F.A. Smith, H.C. Hodge, Toxic effects of fluoride on the rat
729 kidney. I. Acute injury from single large doses, Toxicology and applied pharmacology 3 (1961) 278-89.
730 [33] J.L. Domingo, J.M. Llobet, J.M. Tomas, J. Corbella, Acute toxicity of uranium in rats and mice, Bull
731 Environ Contam Toxicol 39(1) (1987) 168-74.
732 [34] Y. Gueguen, C. Rouas, Données nouvelles sur la néphrotoxicité de l'uranium, Radioprotection
733 47(3) (2012) 345-359.
734 [35] R.W. Leggett, The behavior and chemical toxicity of U in the kidney: a reassessment, Health physics
735 57(3) (1989) 365-383.
736 [36] A.P. Gilman, D.C. Villeneuve, V.E. Secours, A.P. Yagminas, B.L. Tracy, J.M. Quinn, V.E. Valli, R.J.
737 Willes, M.A. Moss, Uranyl nitrate: 28-day and 91-day toxicity studies in the Sprague-Dawley rat, Toxicol
738 Sci 41(1) (1998) 117-28.
739 [37] Y. Gueguen, D. Suhard, C. Poisson, L. Manens, C. Elie, G. Landon, C. Bouvier-Capely, C. Rouas, M.
740 Benderitter, C. Tessier, Low-concentration uranium enters the HepG2 cell nucleus rapidly and induces

741 cell stress response, Toxicology in vitro : an international journal published in association with BIBRA
742 30(1 Pt B) (2015) 552-60.
743 [38] T. Iwakura, Y. Fujigaki, T. Fujikura, N. Ohashi, A. Kato, H. Yasuda, Acquired resistance to rechallenge
744 injury after acute kidney injury in rats is associated with cell cycle arrest in proximal tubule cells,
745 American journal of physiology. Renal physiology 310(9) (2016) F872-84.
746 [39] Y. Gueguen, C. Rouas, A. Monin, L. Manens, J. Stefani, O. Delissen, S. Grison, I. Dublineau,
747 Molecular, cellular, and tissue impact of depleted uranium on xenobiotic-metabolizing enzymes,
748 Archives of toxicology 88(2) (2014) 227-39.
749 [40] M.C. Cardenas-Gonzalez, L.M. Del Razo, J. Barrera-Chimal, T. Jacobo-Estrada, E. Lopez-Bayghen,
750 N.A. Bobadilla, O. Barbier, Proximal renal tubular injury in rats sub-chronically exposed to low fluoride
751 concentrations, Toxicology and applied pharmacology 272(3) (2013) 888-94.
752 [41] Y.G. Long, Y.N. Wang, J. Chen, S.F. Jiang, A. Nordberg, Z.Z. Guan, Chronic fluoride toxicity decreases
753 the number of nicotinic acetylcholine receptors in rat brain, Neurotoxicol Teratol 24(6) (2002) 751-7.
754 [42] Y.M. Shivarajashankara, A.R. Shivashankara, P.G. Bhat, S.H. Rao, Lipid peroxidation and
755 antioxidant systems in the blood of young rats subjected to chronic fluoride toxicity, Indian J Exp Biol
756 41(8) (2003) 857-60.
757 [43] A.R. Shivashankara, Y.M. Shivarajashankara, P.G. Bhat, S.H. Rao, Lipid peroxidation and
758 antioxidant defense systems in liver of rats in chronic fluoride toxicity, Bull Environ Contam Toxicol
759 68(4) (2002) 612-6.
760 [44] M. Cardenas-Gonzalez, T. Jacobo Estrada, R. Rodriguez-Munoz, J. Barrera-Chimal, N.A. Bobadilla,
761 O.C. Barbier, L.M. Del Razo, Sub-chronic exposure to fluoride impacts the response to a subsequent
762 nephrotoxic treatment with gentamicin, Journal of applied toxicology : JAT 36(2) (2016) 309-19.
763 [45] F. Lagarde, C. Beausoleil, S.M. Belcher, L.P. Belzunces, C. Emond, M. Guerbet, C. Rousselle, Non-
764 monotonic dose-response relationships and endocrine disruptors: a qualitative method of assessment,
765 Environmental health : a global access science source 14 (2015) 13.
766 [46] L.E. Feinendegen, A.L. Brooks, W.F. Morgan, Biological consequences and health risks of low-level
767 exposure to ionizing radiation: commentary on the workshop, Health physics 100(3) (2011) 247-59.
768 [47] H. Matsumoto, N. Hamada, A. Takahashi, Y. Kobayashi, T. Ohnishi, Vanguards of paradigm shift in
769 radiation biology: radiation-induced adaptive and bystander responses, Journal of radiation research
770 48(2) (2007) 97-106.
771 [48] G. Olivieri, J. Bodycote, S. Wolff, Adaptive response of human lymphocytes to low concentrations
772 of radioactive thymidine, Science 223(4636) (1984) 594-7.
773 [49] Y. Gueguen, A. Bontemps, T.G. Ebrahimian, Adaptive responses to low doses of radiation or
774 chemicals: their cellular and molecular mechanisms, Cellular and molecular life sciences : CMLS 76(7)
775 (2019) 1255-1273.
776 [50] R.L. Kathren, R.K. Burklin, Acute chemical toxicity of uranium, Health physics 94(2) (2008) 170-9.
777 [51] K.L. Zimmerman, D.S. Barber, M.F. Ehrich, L. Tobias, S. Hancock, J. Hinckley, E.M. Binder, B.S.
778 Jortner, Temporal clinical chemistry and microscopic renal effects following acute uranyl acetate
779 exposure, Toxicologic pathology 35(7) (2007) 1000-9.
780 [52] C. Rouas, J. Stefani, S. Grison, L. Grandcolas, C. Baudelin, I. Dublineau, M. Pallardy, Y. Gueguen,
781 Effect of nephrotoxic treatment with gentamicin on rats chronically exposed to uranium, Toxicology
782 279(1-3) (2011) 27-35.
783 [53] S.G. Emeigh Hart, Assessment of renal injury in vivo, Journal of pharmacological and toxicological
784 methods 52 (2005) 30-45.
785 [54] Y. Gueguen, C. Rouas, F.A. Leblond, Les biomarqueurs d'atteinte rénale, Néphrologie et
786 Thérapeutique 8 (2012) 146-155.
787 [55] S. Hidaka, B. Kranzlin, N. Gretz, R. Witzgall, Urinary clusterin levels in the rat correlate with the
788 severity of tubular damage and may help to differentiate between glomerular and tubular injuries, Cell
789 and tissue research 310(3) (2002) 289-96.
790 [56] T. Ichimura, C.C. Hung, S.A. Yang, J.L. Stevens, J.V. Bonventre, Kidney injury molecule-1: a tissue
791 and urinary biomarker for nephrotoxicant-induced renal injury, American journal of physiology. Renal
792 physiology 286(3) (2004) F552-63.

[57] I. Tanida, T. Ueno, E. Kominami, LC3 and Autophagy, Methods Mol Biol 445 (2008) 77-88.
[58] E.J. Calabrese, L.A. Baldwin, The frequency of U-shaped dose responses in the toxicological literature, Toxicological sciences : an official journal of the Society of Toxicology 62(2) (2001) 330-8.
[59] S. Tapio, V. Jacob, Radioadaptive response revisited, Radiation and environmental biophysics 46(1) (2007) 1-12.
[60] E. Birkner, E. Grucka-Mamczar, Z. Machoy, R. Tarnawski, R. Polaniak, Disturbance of protein metabolism in rats after acute poisoning with sodium fluoride, Fluoride 33(4) (2000) 182-186.
[61] A. Shashi, J. Singh, S. Thapar, Toxic effects of fluoride on rabbit kidney, Fluoride 35 (2002) 38-50.
[62] Y. Sun, Y. Fujigaki, M. Sakakima, A. Hishida, Acquired resistance to rechallenge injury in rats recovered from subclinical renal damage with uranyl acetate--Importance of proliferative activity of tubular cells, Toxicology and applied pharmacology 243(1) (2010) 104-10.
[63] I. Dublineau, M. Souidi, Y. Gueguen, P. Lestaevel, J.M. Bertho, L. Manens, O. Delissen, S. Grison, A. Paulard, A. Monin, Y. Kern, C. Rouas, J. Loyen, P. Gourmelon, J. Aigueperse, Unexpected lack of deleterious effects of uranium on physiological systems following a chronic oral intake in adult rat, BioMed research international 2014 (2014) 181989.
[64] C.A. Kobayashi, A.L. Leite, T.L. Silva, L.D. Santos, F.C. Nogueira, R.C. Oliveira, M.S. Palma, G.B. Domont, M.A. Buzalaf, Proteomic analysis of kidney in rats chronically exposed to fluoride, Chem Biol Interact 180(2) (2009) 305-11.
[65] G. Kroemer, G. Marino, B. Levine, Autophagy and the integrated stress response, Molecular cell 40(2) (2010) 280-93.
[66] V. Pierrefite-Carle, S. Santucci-Darmanin, V. Breuil, T. Gritsaenko, C. Vidaud, G. Creff, P.L. Solari, S. Pagnotta, R. Al-Sahlanee, C.D. Auwer, G.F. Carle, Effect of natural uranium on the UMR-106 osteoblastic cell line: impairment of the autophagic process as an underlying mechanism of uranium toxicity, Arch Toxicol (2016).
[67] M. Schroder, The unfolded protein response, Molecular biotechnology 34(2) (2006) 279-90.
[68] I. Szumiel, Radiation hormesis: Autophagy and other cellular mechanisms, International journal of radiation biology 88(9) (2012) 619-28.
[69] L. Hurault, G. Creff, A. Hagege, S. Santucci-Darmanin, S. Pagnotta, D. Farlay, C. Den Auwer, V. Pierrefite-Carle, G.F. Carle, Uranium Effect on Osteocytic Cells In Vitro, Toxicological sciences : an official journal of the Society of Toxicology 170(1) (2019) 199-209.
[70] W.J. Liu, M.N. Luo, J. Tan, W. Chen, L.Z. Huang, C. Yang, Q. Pan, B. Li, H.F. Liu, Autophagy activation reduces renal tubular injury induced by urinary proteins, Autophagy 10(2) (2014) 243-56.
[71] I. Dublineau, L. Grandcolas, S. Grison, C. Baudelin, F. Paquet, P. Voisin, J. Aigueperse, P. Gourmelon, Modifications of inflammatory pathways in rat intestine following chronic ingestion of depleted uranium, Toxicological sciences : an official journal of the Society of Toxicology 98(2) (2007) 458-68.
[72] A.R. Nair, W.K. Lee, K. Smeets, Q. Swennen, A. Sanchez, F. Thevenod, A. Cuypers, Glutathione and mitochondria determine acute defense responses and adaptive processes in cadmium-induced oxidative stress and toxicity of the kidney, Archives of toxicology 89(12) (2015) 2273-89.
[73] J. Liu, W. Qu, M.B. Kadiiska, Role of oxidative stress in cadmium toxicity and carcinogenesis, Toxicology and applied pharmacology 238(3) (2009) 209-14.
[74] Y. Zhao, Y. Li, J. Wang, R.K. Manthari, Fluoride induces apoptosis and autophagy through the IL-17 signaling pathway in mice hepatocytes, Arch Toxicol 92(11) (2018) 3277-3289.
[75] C.R. Brooks, M.Y. Yeung, Y.S. Brooks, H. Chen, T. Ichimura, J.M. Henderson, J.V. Bonventre, KIM-1-/TIM-1-mediated phagocytosis links ATG5-/ULK1-dependent clearance of apoptotic cells to antigen presentation, The EMBO journal 34(19) (2015) 2441-64.
[76] T. Ichimura, S. Mou, Kidney injury molecule-1 in acute kidney injury and renal repair: a review, Zhong xi yi jie he xue bao = Journal of Chinese integrative medicine 6(5) (2008) 533-8.
[77] M. Sumarac-Dumanovic, D. Stevanovic, A. Ljubic, J. Jorga, M. Simic, D. Stamenkovic-Pejkovic, V. Starcevic, V. Trajkovic, D. Micic, Increased activity of interleukin-23/interleukin-17 proinflammatory axis in obese women, Int J Obes (Lond) 33(1) (2009) 151-6.

845